

Stopping Criterion Design for Recursive Bayesian Classification: Analysis and Decision Geometry

Aziz Koçanaoğulları, Murat Akcakaya, Deniz Erdoğmuş

Abstract—Systems that are based on recursive Bayesian updates for classification limit the cost of evidence collection through certain stopping/termination criteria and accordingly enforce decision making. Conventionally, two termination criteria based on pre-defined thresholds over (i) the maximum of the state posterior distribution; and (ii) the state posterior uncertainty are commonly used. In this paper, we propose a geometric interpretation over the state posterior progression and accordingly we provide a point-by-point analysis over the disadvantages of using such conventional termination criteria. For example, through the proposed geometric interpretation we show that confidence thresholds defined over maximum of the state posteriors suffer from stiffness that results in unnecessary evidence collection whereas uncertainty based thresholding methods are fragile to number of categories and terminate prematurely if some state candidates are already discovered to be unfavorable. Moreover, both types of termination methods neglect the evolution of posterior updates. We then propose a new stopping/termination criterion with a geometrical insight to overcome the limitations of these conventional methods and provide a comparison in terms of decision accuracy and speed. We validate our claims using simulations and using real experimental data obtained through a brain computer interfaced typing system.

Index Terms—Active Learning, Sequential Decision Making, Recursive Bayesian Classification, Optimal Stopping Criterion Design



1 INTRODUCTION

Recursive Bayesian inference for classification (RBC) is beneficial in gradually increasing decision quality by incorporating more evidence into the decision process in situations where data or evidence is acquired sequentially over time. The most recent belief, represented by the latest label posterior probability distribution, is obtained by incorporating new evidence in a Bayesian manner at each update step [1], [2], [3], [4]. The trade-off between decision confidence and evidence acquisition cost is controlled by a stopping criterion that controls when to terminate evidence collection and return an estimated class label. Fundamental components of RBC include: (S) A stopping criterion based on the posterior probability to stop evidence collection; (Q) a querying step to decide how to collect further evidence from relevant sources to benefit speed and accuracy objectives of RBC; (C) an classification objective based on the posterior distribution and loss values attributed to each true label and decision option pair to determine the optimal decision once the stopping criterion has been satisfied. The iterative process can be summarized as follows:

while (S) not satisfied **do** (Q); **return** state with (C)

- Aziz Koçanaoğulları and Deniz Erdoğmuş were with Northeastern University Department of Electrical and Computer Engineering 409 Dana Research Center 360 Huntington Avenue Boston, MA 02115.
E-mail: akocanaoğullari@ece.neu.edu, erdogmus@ece.neu.edu
- Murat Akcakaya was with Pittsburgh University Department of Electrical and Computer Engineering 1238 Benedum Hall Pittsburgh, PA 15261.
E-mail: akcakaya@pitt.edu

This work is supported by NSF (IIS-1149570, CNS-1544895, IIS-1715858, IIS-1717654, IIS-1844885, IIS-1915083), DHHS (90RE5017-02-01), and NIH (R01DC009834).

In this paper, we focus on designing stopping criteria for (S) based on the latest label posterior $p = [p_1, p_2, \dots, p_n]$, which is a categorical probability distribution. In the remainder of this paper, in order to keep the illustrations and derivations simple, we assume that the objective in (C) is to minimize probability of error (therefore 0-1 loss is assumed), thus when a decision is made, it will be based on the maximum a posteriori (MAP) classification rule; that is the then-most-likely-label in the latest posterior will be selected as the decision. The presented approach can be generalized to the more general expected loss minimization classification setting, but is outside the scope of this paper. We also do not discuss different querying strategies, as they too are outside the scope.

The RBC procedure will terminate when the stopping criterion in (S) (namely (S_C)) is met by the current label posterior distribution ($S_C(p) = \text{true}$). The most commonly used approach is to require that a confidence threshold has been exceeded ($S_C(p) = \text{true}$ if $\max_i p_i > \tau$). All label probability distributions p that satisfy S_C form a set called the stopping region $S_R = \{p | S_C(p) = \text{true}\}$. If the posterior distribution falls into this set, the system terminates and a classification-decision is made based on (C). The design of an optimal S_R has been referred to as "optimal stopping criterion design" [5].

In this paper, we focus on the analysis of S_C . Specifically identifying the limitations of conventional confidence thresholding and uncertainty based methods, with the aid of analytical representations that arise from the geometry of the probability simplex, we propose a new perspective for stopping criterion design that enables trading off accuracy for speed in ways not possible with conventional uncertainty

Stopping Region: $S_R := \{p \mathcal{S}_C(p) = \text{true}\}$			
Identifier	Root	Stopping Criterion (\mathcal{S}_C)	Reference
(M1)	Confidence Level	$\max_{\sigma} p(\sigma \mathcal{H}_s) > \tau$	[6]
(M2)	Renyi Entropy ($\alpha = 2$)	$H_{\alpha}(p(\sigma \mathcal{H}_s)) < c_{H_2}$	[7]
(M3)	Shannon's Entropy	$H(p(\sigma \mathcal{H}_s)) < c_H$	[8]
(M4)	Renyi Entropy ($\alpha = 0.2$)	$H_{\alpha}(p(\sigma \mathcal{H}_s)) < c_{H_{0.2}}$	[7]
(M5)	Kullback Liebler Div.	$\delta_{KL}(p(\sigma \mathcal{H}_s), p(\sigma \mathcal{H}_{s-1})) < c_{\delta_{KL}}$	[9]

TABLE 1: Conventional stopping criteria, here $c_s \in \mathbb{R}$ denote the limits of the criteria. These methods are further used in the experiments section with the respective identifiers as a baseline to the proposed perspective of the stopping method. Limiting criterion \mathcal{S}_C defines a set with all distributions p that satisfy the condition. In recursive estimation, if the posterior probability becomes an element of the set, the system terminates to make an inference/classification.

methods. In particular, as illustrated in Fig.1(c), we propose to bend the stopping region to enable early decisions, especially in situations where there is no strong contender to the top decision choice (posterior moving from the middle region in the simplex), but not when there is a strong second contender option (posterior moving from near the edges in the simplex). In numerical experiments, we demonstrate that this strategy enables significant inference speed-up with negligible increase in expected loss.

Problem Formulation and Related Work

Let class label σ be an element of a finite set \mathcal{A} . We refer to each iteration in RBC as a *sequence*, indexed by $s \in \mathbb{N}$. Each sequence may include a set of measurements acquired in response to queries $\Phi_s \triangleq \{\phi_s^1, \dots, \phi_s^N\}$, where N denotes number of queries. These measurements provide evidence (raw data or processed features) $\varepsilon_s \triangleq \{\varepsilon_s^1, \dots, \varepsilon_s^N\}$ conditioned on the queries, and the true label. RBC posterior updates use this evidence. For notation simplicity, we use $\mathcal{H}_s \triangleq \{\varepsilon_{1:s}, \Phi_{1:s}, \mathcal{H}_0\}$ to represent the combination of all evidence collected in sequences 1 to s , as well as the prior, \mathcal{H}_0 . RBC steps (assuming MAP classification rule) are:

$$\begin{aligned}
 (S) : \quad & p(\sigma | \mathcal{H}_s) \in (\mathcal{S}_R := \{p | \mathcal{S}_C(p) = \text{true}\}) \\
 (C) : \quad & \hat{\sigma} = \arg \max_{\sigma \in \mathcal{A}} p(\sigma | \mathcal{H}_s) \\
 (Q) : \quad & \Phi_{s+1} \rightarrow \varepsilon_{s+1} \text{ with the anticipated joint} \\
 & p(\sigma | \mathcal{H}_{s+1}) = p(\sigma | \mathcal{H}_s) \frac{p(\varepsilon_{s+1} | \sigma, \Phi_{s+1})}{p(\varepsilon_s | \Phi_{s+1})}
 \end{aligned} \tag{1}$$

In this paper we focus on (C) The most common \mathcal{S}_C is thresholding the highest value in the latest posterior by τ [6], [10]: $\mathcal{S}_C(p) = \text{true}$ if $\max_i p_i > \tau$. This rule directly enforces that a decision is made with a prespecified confidence level, and does not consider the distribution of probability mass among other options. To minimize false alarm rate, the threshold is usually set to a large number. Furthermore, this entangles early stopping options and leads to further redundant evidence collection [11]. Relaxation of stiffness of posterior thresholding is possible with information theoretic objectives. Uncertainty measures, including Shannon entropy [12], can be used to have termination based on the spread of posterior probability mass. Golovin [9] uses Shannon entropy as a stopping criterion: " $\mathcal{S}_C(p) = \text{true}$ if $H(p) < c_H$ ". Yingzhen [13] and Igal [7] use Renyi entropy: " $\mathcal{S}_C(p) = \text{true}$ if $H_{\alpha}(p) < c_{H_{\alpha}}$ ". Uncertainty based stopping criteria based on Renyi entropy $H_{\alpha}(p)$ family with $\alpha \geq 0$ includes, as special cases, Shannon entropy (in the limit as $\alpha \rightarrow 1$), and confidence thresholding (in the limit

as $\alpha \rightarrow \infty$) methods. In contrast to these uncertainty based stopping criteria, With a diminishing-returns perspective, Weinshall [14] and Geisser [8] apply a threshold to the Kullback-Leibler (KL) divergence between two consecutive posterior distributions to terminate evidence collection: " $\mathcal{S}_C(p) = \text{true}$ if $D_{KL}(p_s || p_{s-1}) < c_{D_{KL}}$ ". Pavlichin [15] proposes a chained-KL divergence to monitor posterior progression in the probability simplex. Banerjee [16] proposes using Bregman divergences in the context of clustering. All of these stopping criteria focus on how far the posterior is from the uniform distribution that is at the center of the probability simplex, as opposed to assessing how close the posterior to a vertex of the simplex (corresponding to a one-hot distribution) [17]. In this paper, we discuss the limitations of these criteria summarized in Table 1, and propose a new family of stopping criteria, then illustrate theoretically, and with numerical examples and experiments, the benefits of the proposed approach.

Contributions

We introduce a geometrical representation for recursive Bayesian classification and show that: (i) uncertainty based methods are sensitive to the number of possible classes, and (ii) they ignore the posterior update trajectory in the recursive classification task. Using (i) and (ii) together, we show that the stopping regions defined based on uncertainty methods diverge from the region formed by confidence threshold defined over the posterior distribution resulting in decrease in classification accuracy. We then propose a new stopping criterion design perspective that is not only robust to number of classes but also defines a stopping region that is inline with the progression of the posterior update. We show that such a perspective not only increases the classification speed by decreasing redundant evidence collection caused by the stopping regions defined through the confidence level thresholds, but also maintains a high classification accuracy by limiting false positive rate. We also provide a practical use case for the design. Specifically, we consider a brain computer interface typing system. Detailed demonstrations and proofs of the analytical results are provided in the appendix Sec. 7.4 for neat presentation.

2 PROBLEM GEOMETRY

To promote the representative power of visualization, in this paper we use information geometric representation of recursive classification problem [18]. As will be discussed,

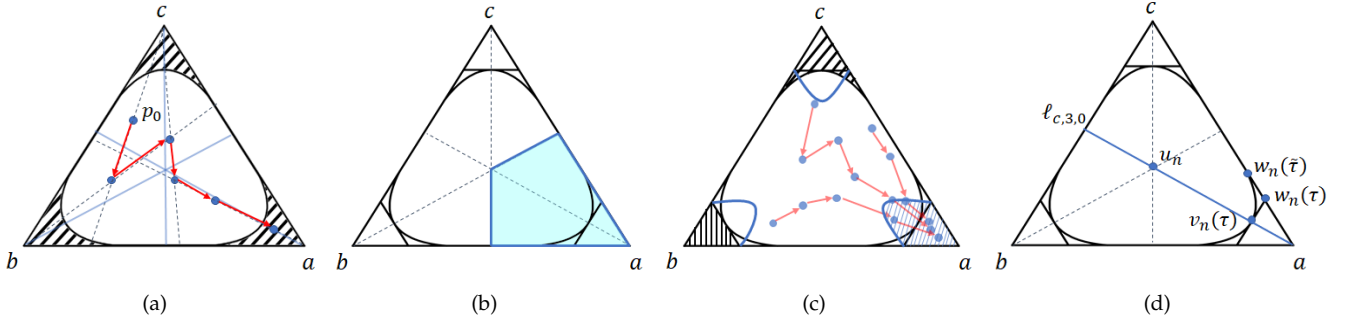


Fig. 1: Decision geometry for recursive classification where true class is a . (a) The initialization of the system with a prior information and (S) region. The system terminates once the posterior yields within the (S) region (dashed). (b) Decision region for ' a ' enforced by (C) . (c) Three different perspectives in S_R design, we want to tilt the boundary to achieve early stopping. (d) The origin of the simplex u_n and special points defined in (3). Equi-entropy contours and corresponding posterior threshold lines are in solid black. The intersection point is at v_n (See Obs.1).

this representation allows us to represent progression of the posterior probability distribution $p(\sigma|\mathcal{H}_s)$ as the evidence collection steps s increases and to introduce a mean for analytical reasoning for stopping criterion \mathcal{S}_C design. We use simplex as a domain for probability distributions;

$$\Delta_n = \{(p_1, p_2, \dots, p_n) \in \mathbb{R}^n | p_i > 0 \forall i, \sum_i p_i = 1\} \quad (2)$$

Here Δ_n represents the set that includes categorical probability distributions, where the simplex is an $n - 1$ dimensional geometrical object in \mathbb{R}^n . We visualize an example simplex for a category with 3 elements in Fig.1. To preserve neat visualization, we interpret our reasoning using the triangle throughout the paper, but all the results can be generalized to n -dimensional case without loss of generality. Moreover, we use the following addition operation that allows us to represent posterior updates;

Addition: Given $p, q \in \Delta_n$ the addition operation is defined as:

$$p \oplus q = \frac{[p_1 q_1, p_2 q_2, \dots, p_n q_n]}{\sum_i p_i q_i}$$

Observe that addition satisfies the Bayes' theorem: $p(\sigma|\varepsilon) = p(\sigma) \oplus p(\varepsilon|\sigma)$ which allows us to represent the evolution of the posterior distribution using the addition operation within the simplex. For algebra to work $p(\varepsilon|\sigma)$ does not need to be unit ℓ_1 norm and hence $\notin \Delta_n$, but what we interpret here is the normalized vector over σ even algebraically \oplus is applicable. Rigorous definition of this simplification is shown in the appendix Sec.7.1. The zero element in Δ_n is denoted by u_n being the uniform distribution as shown in Fig.1(d).

Proposition 1 ([19]). *Simplex $\{\Delta_n | \oplus, \otimes\}$ forms a vector space.*

In the presence of a prior distribution, recursive classification starts with a distribution probably different than uniform distribution as presented in Fig.1-(a). To make a correct decision, the posterior for respective element is required to be the most likely (e.g. the region for a is highlighted in Fig.1-(b)). Through evidence collections, the posterior distribution moves within the simplex visualized in Fig.1-(c) that is algebraically denoted with \oplus above. (S) criterion forms the decision lines within the simplex and the inequality condition covers the area of evidence collection termination that are visualized by dashed areas in Fig.1. Once the posterior probability distribution reaches that area, the system

terminates evidence collection, makes an inference outputs the classification decision.

3 CONVENTIONAL STOPPING CRITERIA

In this section we discuss the limitations of the conventional methods that are used for stopping criteria \mathcal{S}_C design. Consider the following 2 motivating examples assuming 10 class classification problems;

example1: $p, q \in \Delta_{10}$ with $p = [.6, .4 - 8\epsilon, \epsilon, \dots]$ where $0 < \epsilon < 1$ and $q = [.7, .03, \dots]$. It is apparent that q is a better stopping point to decide on the 1st element as the classification result. However, if Shannon's entropy is used to measure the distance from uniform distribution u_n , and accordingly utilized as a stopping criterion, then $0.97 \approx H(p) < H(q) \approx 1.82$. This means that the evidence collection would have been terminated when p is reached. Hence, the uncertainty based (S) suffers from not taking the probability mass index of interest into consideration.

example2: $p, q \in \Delta_{10}$ with $p1 = [.5, .5 - 8\epsilon, \epsilon, \dots]$, $p2 = [.6, .4 - 8\epsilon, \epsilon, \dots]$ where $0 < \epsilon < 1$ and $q1 = [.5, 0.05, \dots]$, $q2 = [.6, 0.04, \dots]$ and we compare ps then qs . Even the confidence level on a particular class differs the same amount .1, for ps the 2nd best class is still a legit competitor, whereas for qs there was no other competitor. Here even though qs are in a more central position in the simplex than ps they provide a higher confidence in classification. However, ps are close to the edge of the simplex and accordingly may result in the termination of the evidence collection before more confident posterior qs can be achieved. This means that the location of posteriors in Δ_n matters and with an appropriate design of stopping criterion, the system evidence collection could be stopped when the confidence on the classification is higher.

In this section we analytically show what these examples mean for the stopping criterion (\mathcal{S}_C) design.

3.1 Frail Confidence

The confidence behavior of uncertainty based methods are similar. Shannon entropy on the other hand is the most commonly used and hence in this section we specifically

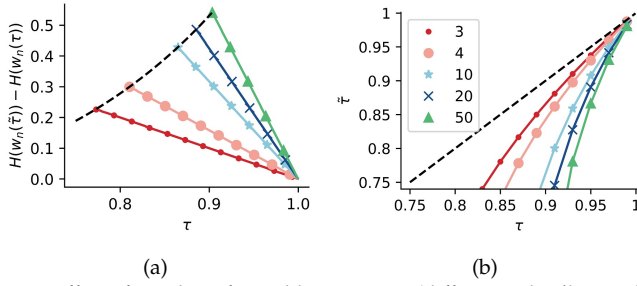


Fig. 2: Effect of number of possible categories (different color/line codes) on the decision boundary. (a) represents the difference between entropy values of the probabilities v_n, w_n for a given confidence level τ . (b) represents the τ and $\tilde{\tau}$ values where $H(w_n(\tilde{\tau})) = H(v_n(\tau))$.

focus on (M3), as defined in Table.1. We refer the reader to the appendix Sec.7.2 for decision boundary similarities between (M2)-(M3) and (M4). To point out the relationship between the confidence in classification and entropy based stopping region $S_R(H(\cdot)) := \{p | H(p) < c_H\}$ (M3) we define two special probability points in Δ_n :

$$\begin{aligned} v_n(\tau) &= \left[\tau, \frac{1-\tau}{n-1}, \dots, \frac{1-\tau}{n-1} \right] \\ w_n(\tau) &= [\tau, 1-\tau, 0, \dots, 0] \end{aligned} \quad (3)$$

Here, $v_n(\tau)$ corresponds to distributions where one class has likelihood of τ and the others share the remaining probability uniformly, $w_n(\tau)$ corresponds to distributions where only two class exist with probability values $\tau, 1-\tau$. These definitions are also visualized in Fig.1(d).

In this paper, we bundle the uncertainty and confidence τ via $\tau' = H(v_n(\tau))$. We show the following weak points: $H(\cdot)$ is sensitive to n and τ , and $H(\cdot)$ conflicts with the inference step (C) of Eqn. (1) for a given set of parameters. To analyze these, we introduce the relationship between confidence and entropy \mathcal{S}_{CS} with the help of (3). We state for a confidence τ that entropy achieves its maximum value at the point $v_n(\tau)$ and for an equi-entropy contour with value of $H(v_n(\tau))$ maximum achievable confidence is τ . See the following proposition.

Proposition 2. For a defined confidence level τ ;

$$\begin{aligned} C_\tau &= \{p | \max_i p_i = \tau\} \implies \max_{p \in C_\tau} H(p) = H(v_n(\tau)) \\ S_\tau &= \{p | H(p) = H(v_n(\tau))\} \implies \max_{p \in S_\tau} \max_i p_i = \tau \end{aligned}$$

Observation 1. Following descriptions in Proposition 2, confidence line for τ , C_τ , intersects with the equi-entropy contours, S_τ , only at $v_n(\tau)$ points.

Following this observation, we state that the set between the corners of the simplex Δ_n and C_τ is a subset of the set between the corners and S_τ as presented in the following observation:

Observation 2. Define $S_1 = \{p | \max_i p_i \geq \tau\}$ and $S_2 = \{p | H(p) \leq \tau'\}$, $\tau' = H(v_n(\tau))$, $\forall \tau \in [1/n, 1]$ then $S_1 \subset S_2$. Therefore the (S) region designed by entropy S_1 is larger than the region designed with the confidence threshold S_2 .

It is apparent that the stopping region defined by entropy (M3) is larger than the stopping region defined through confidence level (M1) and hence enlarging the \mathcal{R}_S in (1). This increase in the region, on the other hand, decreases

confidence. To analyze it we need to find the minimum confidence in an equi-entropy contour. It is shown that the minimum confidence is attained at $w_n(\tilde{\tau})$ that satisfies the following:

Observation 3. [20]

$$\begin{aligned} H(v_n(\tau)) &< 1, S_\tau = \{p | H(p) = H(v_n(\tau))\} \\ \text{then } \min_{p \in S_\tau} \max_i p_i &= \tilde{\tau} \\ \text{s.t. } -\tilde{\tau} \log_2(\tilde{\tau}) - (1-\tilde{\tau}) \log_2(1-\tilde{\tau}) &= H(v_n(\tau)) \end{aligned}$$

This observation states that the entropy based (S) boundary attains the minimum required max-probability value $\tilde{\tau}$ at $w_n(\tilde{\tau})$. $\tilde{\tau}$ vs τ and entropy values difference between $w_n(\tau)$ and $w_n(\tilde{\tau})$ are presented in Fig.2 for changing number of categories in the classification. Observe from Fig.2 that entropy is fragile with respect to the number of classes and the difference between $\tilde{\tau}$ and τ increases by decreasing values of τ . Also observe that $H(w_n(\tilde{\tau})) - H(w_n(\tau))$ decreases linearly with τ , and increases exponentially (dotted-line) with n as presented in Fig.2(a).

By nature, uncertainty based (S) is capable of returning a class label when the confidence of the class is low as shown in Obs.3. If there exists no $\tilde{\tau}$ that satisfies Obs.3, equi-entropy contours do not intersect with the simplex boundary. This condition might result in immediate stopping if one of the classes is already unfavorable as shown in Fig.3(a) with the trajectories close to $[a, c]$ edge.

The above Proposition 2, and Observations 1-3 show that under certain conditions, the regions defined by uncertainty criteria may significantly diverge from the region formed by the confidence level threshold that was defined over the posterior distribution. To avoid such drawbacks, the system might be set to a high confidence level (e.g. $\tau \approx .95$), such termination already mandates system continue with redundant recursions of evidence collection to achieve high confidence. Accordingly, despite their differences, uncertainty based stopping (M3) and constant confidence threshold (M1) yield similar performances in recursive classification tasks. To analyze these similarities in the classification performances, in the next section, we investigate the behavior of the posterior motion over the probability simplex. Through such an analysis, we then gain an insight into designing stopping criterion that will avoid high confidence levels and corresponding redundant recursions/evidence collections.

3.2 Posterior Motion

In this section we assume the posterior probability of the true state/class increases on average [21] and with such an assumption we show that there exists a particular trajectory for the posterior motion. With such an insight, we reason the similar operation behavior of constant threshold and uncertainty based stopping criteria. Moreover, this analysis will further provide us insight into relaxing stopping region S_R considering the trajectory for early stopping.

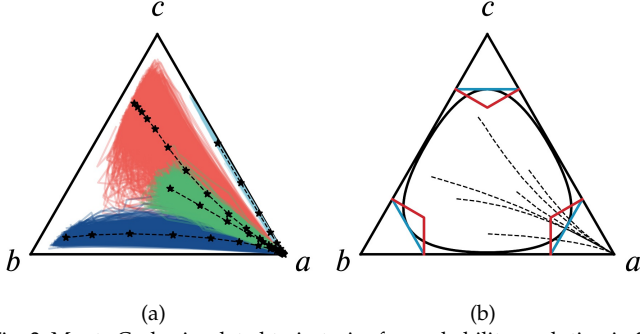


Fig. 3: Monte Carlo simulated trajectories for probability evolution in 3D simplex. To simulate the trajectories we sample evidence from lognormal distributions. (a) Each color represent 100 simulated examples from a different starting point and dashed lines representing the means of the trajectories. Observe the case where one of the classes is already disfavored (one between a, c), if decision boundary does not intersect with the edge, that results in immediate termination. (b) Three different perspectives for S_R design. We observe that the behavior of entropy (black) and confidence threshold (blue) are similar if trajectories are considered. In the method section we propose a region design using an equi-distance curves wrt. to the corners (red).

Given a prior point $p(\sigma)$, the posterior evolution with given pairs of queries and evidences (Φ, ε) is given by the following:

$$p(\sigma|\Phi_{0:s}, \varepsilon_{0:s}) = p(\sigma) \oplus p(\varepsilon_1|\sigma, \phi_1) \oplus \dots \oplus p(\varepsilon_s|\sigma, \phi_s)$$

The trajectory of the posterior distribution is determined by the evidence likelihood $p(\varepsilon_s|\sigma, \phi_s)$ at each step s and the evidence collected through query ϕ_s . In this section we assume two noisy information channels for true class and incorrect class respectively. Once the true class is queried, evidence is sampled from the "positive" distribution and evidence is sampled from "negative" distribution otherwise. In this section we show that the trajectory of the posterior distribution follows a central path as it gets closer to the corner of interest as shown in Fig.3-(b). To show this relationship we first analyze the behavior of the posterior when evidence corresponding to a single query is observed. **Lemma 1.** Let $a \in \mathcal{A}$ and let $\phi(a)$ denote the query related with state a then $p(\sigma) = [p_1 = p(a), p_2, \dots, p_n]$. $p(\sigma)$, $[1, 0, \dots, 0]$ and $p(\sigma) \oplus p(\varepsilon|\sigma, \phi(a)) \forall \varepsilon, \forall p(\sigma)$ are collinear.

Hence, once the system queries the environment, posterior probability for classification takes a step on the line that passes through the current position and the corner addressed by query. Moreover, on average, if the query addresses true state, the posterior moves towards the respective corner, if the query addresses an incorrect estimate the posterior moves away from the respective corner. To show that in general posterior gets closer to a central position, we need the projection of a posterior point to the line that passes through the center (u_n) and one of the corners.

Lemma 2. Given $p(\sigma) = p = [p_1, p_2, \dots, p_n] \in \Delta_n$ and given the line $\ell_{c_n, i=1} = \{[\tau, \frac{1-\tau}{n-1}, \dots, \frac{1-\tau}{n-1}] | \forall \tau \in [0, 1]\}$ then ℓ_2 norm projection of point $p(\sigma)$ onto line $\ell_{c_n, i=1}$ is the following:

$$\begin{aligned} \text{proj}_{\ell_{c_n, i=1}}(p(\sigma)) &= \arg \min_{p \in \ell_{c_n, i=1}} \|p(\sigma) - p\|_2 \\ &= \left[p_1, \frac{1-p_1}{n-1}, \dots, \frac{1-p_1}{n-1} \right] \end{aligned}$$

To give an example, line $\ell_{c_n=3, i=1}$ is visualized in Fig.1(d) where 1st location is a . With this projection operation we show that ℓ_2 -norm distance between the projection and the actual point d_s at sequence s decreases quadratically with respect to the posterior as s increases. This statement is given in the following proposition:

Proposition 3. Following Lemma 2, given $p(\sigma) \in \Delta_n$:

$$\|p(\sigma) - \text{proj}_{\ell_{c_n, i=1}} p(\sigma)\|_2^2 \propto (1 - p_1)^2$$

Following this, one defines the reduction between two sequences,

$$\exists \hat{s} \text{ s.t. } \|p(\sigma|\mathcal{H}_s) - \text{proj}_{\ell_{c_n, i=1}} p(\sigma|\mathcal{H}_s)\|_2 = d_s$$

where $\tilde{p}(\sigma|\mathcal{H}_s + 1) = p(\sigma|\mathcal{H}_s) \oplus E_\varepsilon(p(\varepsilon|\sigma, \phi)) \forall \phi$

$$\|\tilde{p}(\sigma|\mathcal{H}_{s+1}) - \text{proj}_{\ell_{c_n, i=1}} \tilde{p}(\sigma|\mathcal{H}_{s+1})\|_2 = d_{s+1}$$

Using Lemma 1 $\implies d_s > d_{s+1} \forall s \geq \hat{s}$

In recursive classification, on average, probability of the true state/class increases sequentially and following the proposition, the posterior probability gets closer to the line that passes through the respective corner and the center. We visualize examples of average trajectories in Fig.3(a). Such a behavior of the posterior distribution describes why the uncertainty and confidence level based stopping criteria behave similarly for high confidence thresholds. Note that both of these methods may suffer from redundant recursions/evidence collections in such cases. On the other hand, observe that, the design of S_R should be inwards towards the center to capture the motion to enable possible early stopping as can be seen from Fig.3(b). Next, based on this observation, we propose a new stopping criterion perspective.

4 PROPOSED PERSPECTIVE

In this section we propose another insight for \mathcal{R}_S design. In the previous section we argued equi-entropy contours formed for (M3) are centered around u_n . Moreover (M3) is sensitive to number of categories and stagger in cases where some of the classes are already unfavorable. Additionally we presented in Figure3-(b) (M3) bends (M1) from the edges to provide early stopping. However, our insight from posterior motion guides us to bend (M1) from the center towards u_n an example is shown in Figure3-(b) by red boundary. Trivially, it is possible to form this by equi-distant points to the respective corners. However, by definition, edges and corners are $\notin \Delta_n$ (represents ∞ [19]) which prevents measuring the distance with conventional information theoretic approaches. To avoid this, exploiting $\Delta_n \subset \mathbb{R}^n$, one can use a distance measure δ defined over \mathbb{R}^n (e.g. ℓ_p norms) and intersect the $\bar{\tau}$ ball around p $B_{\delta}^{\bar{\tau}}(p) = \{x | \delta(p, x) < \bar{\tau}\}$ with Δ_n to obtain $\tilde{B} = B \cap \Delta_n$ centered around a corner and $\in \Delta_n$ $\tilde{B}_{\delta}^{\bar{\tau}}(p) = \{x | \delta(p, x) < \bar{\tau}, x \in \Delta_n\}$. Let $c^k \in \Delta_n$ be the k^{th} corner (e.g. $c^1 = [1, 0, \dots, 0]$), decision region with δ and $\bar{\tau}$ is defined as;

$$S_R : p \in \bigcup_{k \in \{1, 2, \dots, n\}} \tilde{B}_{\delta}^{\bar{\tau}}(c^k) \quad (4)$$

We use a distance measure influenced by Kittler's work [22]: the *delta* divergence. We use the definition of *delta*-

divergence and modify it to define our novel decision region. This divergence determines an interest set (e.g. indices of the most probable elements in respective distributions) and compare the probability mass in these elements. We limit the set to two elements in our paper. The corresponding distance between $p, q \in \Delta_n$ is denoted as δ_{MP} (MP indicating ‘method proposed’) defined as the following;

$$\begin{aligned} \delta_{MP}(p, q) &= \sum_{i \in I} |p_i - q_i|, \quad I = \{j_1, j_2, k_1, k_2\} \\ j_1 &= \arg \max_i p_i, \quad j_2 = \arg \max_{i \neq j_1} p_i \\ k_1 &= \arg \max_i q_i, \quad k_2 = \arg \max_{i \neq k_1} q_i \end{aligned} \quad (5)$$

Observe the measure satisfies non-negativity, identity of indiscernibles and symmetry. Using this distance to obtain balls, we can state the following proposition about the stopping region and criterion, S_R and S_C respectively;

Proposition 4 (Proposed S_R (MP)). c^k being k^{th} corner, $p \in \Delta_n, \delta = \delta_{MP}, \bar{\tau} \in [1/n, 1]$ then;

$$\begin{aligned} S_R : p &\in \bigcup_{k \in \{1, 2, \dots, n\}} \tilde{B}_{\delta}^{\bar{\tau}}(c^k) \\ &\equiv S_C : p_{j_1} - p_{j_2} > 1 - \bar{\tau} \\ \text{where } j_1 &= \arg \max_i p_i \text{ and } j_2 = \arg \max_{i \neq j_1} p_i \end{aligned} \quad (6)$$

We denote this method by (MP). We visualize an example decision boundary in Figure3-(b). As can be observed from the figure, respective decision boundary is inline with the motion of the probability distribution. To have a decision boundary bending the boundary at τ for (M1) from its center the following condition is required;

Observation 4. Given $\bar{\tau} = 2 - 2\tau$ and WLOG for $p \in \Delta_n$, $\arg \max_i p_i = 1$. Define (MP) and (M1) decision boundaries;

$$\begin{aligned} C_{\tau} &= \{p | p_1 = \tau\} \\ B_{\bar{\tau}} &= \{p | p_1 - p_m = 1 - \bar{\tau}, m = \arg \max_{i \neq 1} p_i\} \end{aligned}$$

$$\implies C_{\tau} \cap B_{\bar{\tau}} = w_n(\tau) \text{ and } \max_{p \in B_{\bar{\tau}}} \max_i p_i = \tau$$

Observation 5.

$$\begin{aligned} B_{\bar{\tau}} &= \{p | p_1 - p_m = 1 - \bar{\tau}, m = \arg \max_{i \neq 1} p_i\} \\ \min_{p \in B_{\bar{\tau}}} \max_i p_i &= \frac{1 + (n-1)(1 - \bar{\tau})}{n} = \psi, p = v_n(\psi) \end{aligned}$$

The closest point of the decision boundary to u_n is $v_n(1 + \bar{\tau}((1-n)/n))$ and hence on the line $\ell_{c_n, i}$ for each respective corner i . This implies, unlike uncertainty methods, proposed boundary does not interfere with the inference, (c) function. By definition (5) is robust to number of categories and the cases where one of the classes is already unfavorable. We omit derivations and refer the reader to [22].

Proposition 5. Given $\tau, p = [p_1, p_2, \dots, p_n] \in \Delta_n$ s.t. $2 = \arg \max_{i \neq 1} p_i$ and $p_2 \geq (1 - p_1)\tau$ and evidence $\varepsilon = [\varepsilon_+, 1, \dots, 1]$ where $\varepsilon_+ \sim \text{lognorm}(\mu, c^2)$, we define the

posterior at sequence s $p^s = p^0 \oplus \varepsilon \oplus \dots \oplus \varepsilon$. With $\bar{\tau} = 2 - 2\tau$ and $\tilde{\tau} = ((2\tau - 1)(n - 1) + 1)/n$ define;

$$\begin{aligned} S_{r(M1)} &= \{p^s | p_1^s \geq \tau\} \\ S'_{R(M1)} &= \{p | p_2 \geq \tau\} \\ S_{R(MP)} &= \{p^s | p_1^s - p_2^s \geq 1 - \bar{\tau}\} \\ S'_{R(MP)} &= \{p^s | p_2^s - p_j^s \geq 1 - \bar{\tau}, j = \arg \max_{k \notin \{1, 2\}} p_k^s\} \implies \\ p(p^s \in S_{R(MP)}(p_1, p_2, \bar{\tau}, s)) &\geq p(p^s \in S_{R(M1)}(p_1, \tau, s)) \text{ \& } \\ p(p^s \in S'_{R(M1)}(p_1, p_2, \bar{\tau}, s)) &\geq p(p^s \in S'_{R(MP)}(p_1, p_2, \bar{\tau}, s)) \\ &\geq p(p^s \in S'_{R(M1)}(p_1, p_2, \tau, s)) \quad \forall s \in \{1, 2, \dots\} \end{aligned}$$

Proposition 5 demonstrates that compared to a stopping criterion based on posterior distribution thresholding (M1), the proposed method (MP) always has higher probability of entering the stopping region with correct decision, while the probability of entering an incorrect region resulting in incorrect decision is constrained within certain probability values. Therefore, a system can be designed to achieve a desired true positive probability while limiting false alarm probability by using the proposed stopping criterion. Supporting numerical examples are in the appendix Sec.7.3.1.

5 EXPERIMENTS AND RESULTS

In this section we run experiments to support our findings. Throughout this section we denote the *proposed method* introduced in Section4 by (MP) and compare it with the methods presented in Table1. Specifically, we designate a confidence level τ for (M1). We select respective c s for (M2:4) such that (M1:4) intersect at $v_n(\tau)$. We select $\bar{\tau}$ for (MP) following Obs.4. For (M5) $c_{\delta_{KL}}$ is selected as 10^{-2} . We demonstrate results for the two following cases: (i) Synthetic experiments (ii) A letter decision for electroencephalography (EEG)-based brain computer interface (BCI) typing system.

5.1 Synthetic Experiments

In this section, we present synthetic toy examples to support our propositions in Section 4 that states: proposed method (MP) is robust to prior distributions with disfavored classes and (MP) stops earlier by sacrificing marginal accuracy as it is coherent with the motion of the posterior.

- 1) In the presence of disfavored classes, where the recursive classification is happening in a lower dimension than the cardinality of the class space (e.g. at least one of the class probabilities ≈ 0), uncertainty based methods (especially Renyi Entropy with orders $\alpha \leq 1$) suffer from immediate or rushed stopping (this was discussed in Section 3.1)
- 2) As the cardinality of the class space increases the case described in 1 becomes more drastic.
- 3) Proposed method (MP) in the case of 1 and 2, behaves similar to the confidence thresholding methods. Moreover, (MP) provides an early stopping with marginal accuracy loss when the trajectory follows a central path. (this was discussed in Section 3.2)



$$p(\text{cat}) = 0.42$$

$$p(\text{lion}) = 0.55$$

$$\text{s.t. } |\mathcal{A}| = 10$$

Method		Number of Sequences						
		1	2	3	4	5	6	7
MP	p_{stop}	0.00	0.06	0.22	0.43	0.59	0.67	0.77
	$p_{\text{true stop}}$	0.00	0.67	0.86	0.96	0.97	0.98	0.99
M1	p_{stop}	0.00	0.06	0.22	0.43	0.59	0.67	0.77
	$p_{\text{true stop}}$	0.00	0.67	0.86	0.96	0.97	0.98	0.99
M2	p_{stop}	0.00	0.08	0.27	0.47	0.62	0.70	0.79
	$p_{\text{true stop}}$	0.00	0.67	0.85	0.95	0.95	0.97	0.98
M3	p_{stop}	0.00	0.34	0.56	0.70	0.80	0.85	0.90
	$p_{\text{true stop}}$	0.00	0.20	0.48	0.63	0.74	0.80	0.87
M4	p_{stop}	1.00	1.00	1.00	1.00	1.00	1.00	1.00
	$p_{\text{true stop}}$	0.00	0.55	0.72	0.82	0.87	0.90	0.94
M5	p_{stop}	0.00	0.00	0.37	0.41	0.46	0.55	0.66
	$p_{\text{true stop}}$	0.00	0.00	0.58	0.76	0.87	0.91	0.95
M1	p_{stop}	0.00	0.16	0.37	0.56	0.71	0.77	0.84
	$p_{\text{true stop}}$	0.00	0.64	0.84	0.93	0.95	0.97	0.98

TABLE 2: A toy example with 3 class recursive classification. The set contains "cat, lion, dog" whereas the prior information for the given image (left) is $p = [0.42, 0.55, 0.03]$ with $\tau = .8$. Observe this case directly corresponds to disfavoring a particular class. We proceed in the recursive classification with evidence $\varepsilon = [\varepsilon_+, \varepsilon_-, \varepsilon_-]$ where $\varepsilon_+ \sim \text{lognorm}(0.6, 0.5^2)$ and $\varepsilon_- \sim \text{lognorm}(0, 0.5^2)$. We perform 5000 MC simulations to report each number. On the table (right), we present probability of stopping with the given criteria and accuracy among times the system stopped. As expected entropy (M3) staggers by stopping 34% and with only 20% accuracy within second sequence. More importantly, as we reasoned before, Renyi entropies with order $\alpha < 1$ (M4), $\alpha = 0.2$ in this case, create ambiguous decision regions which leads to stopping all the time as presented. (imagesrc:https://www.amazon.com/Pet-Krewe-PK00101-Costume-Small/dp/B010E4TAKW)

In addition to the methods presented in the main paper, we also use a confidence lower bound with a confidence level $\bar{\tau}$ that is derived in Observation 5 (e.g., $\bar{\tau}$ for which the minimum accuracy can be achieved as (MP)) and we represent this method with (M1). To be precise, for (M1) and (MP) presented in Fig. 3-(b), ($\bar{M}1$) will be the confidence lines each intersect with (MP) at the respective peak points. By design, we expect to show that (MP) is as robust as (M1) and (MP) reaches the speed of ($\bar{M}1$) with marginal accuracy decrease. In our experiments we present scenarios with pre-defined prior information and evidence $\varepsilon = [\varepsilon_+, \varepsilon_-, \varepsilon_-]$ such that ε_+ and ε_- are sampled from lognormal distributions (specifications are listed under each Table 2, 3, 4). In these tables, we report two measures for each method given number of sequences such that p_{stop} represents the probability of stopping, $p_{\text{true|stop}}$ represents the accuracy among all terminations (e.g. $p_{\text{true|stop}} = 0.5, p_{\text{stop}} = 0.6$ means the system correctly selected 300 out of 600 terminated in 1000 Monte Carlo simulations). We highlight the first sequence that achieves $p_{\text{stop}} \geq .5$ indicating a reasonable stopping operational point of a method. Table 2 and Table 3 collectively explain items (1)-(2) such that, in both these tables, it is apparent that (M3) - (M4) perform poorly due to their behavior with disfavored classes. Priors with disfavored classes lead to a trajectory that follows a path closer to sides of the simplex and hence result in rushed and immediate stopping yielding probability of stopping ≈ 1 even in the first few sequences with extremely low accuracy. Observe that (M3) characteristics gets closer to (M4) in Table3 compared to Table2 because of an increase in class space cardinality (as also discussed in the manuscript Figure2-(a)). Table 4 demonstrates a case where the prior is more centric and hence the posterior follows a more central path. Analogous with the previous discussions, uncertainty based methods and confidence thresholding behave similar. In such scenarios (MP) achieves similar accuracy performance compared to competitors but stops 1 sequence earlier.

To summarize the findings, we visualize time accuracy trade-off for each method for the cases presented in Tables 3 and 4.



$$p(\text{cat}) = 0.13$$

$$p(\text{lion}) = 0.52$$

$$p(\text{dog}) = 0.30$$

$$\text{s.t. } |\mathcal{A}| = 10$$

Method	Number of Sequences									
	1	2	3	4	5	6	7	8	9	
MP	p_{stop}	0.00	0.08	0.26	0.42	0.61	0.70	0.78	0.82	0.88
	$p_{\text{true stop}}$	0.00	0.36	0.78	0.89	0.94	0.96	0.97	0.98	0.98
M1	p_{stop}	0.00	0.03	0.18	0.35	0.54	0.66	0.76	0.81	0.86
	$p_{\text{true stop}}$	0.00	0.29	0.83	0.90	0.94	0.97	0.97	0.98	0.98
M2	p_{stop}	0.00	0.05	0.23	0.41	0.61	0.72	0.81	0.85	0.88
	$p_{\text{true stop}}$	0.00	0.32	0.80	0.89	0.94	0.96	0.97	0.98	0.98
M3	p_{stop}	1.00	1.00	1.00	1.00	1.00	1.00	1.00	1.00	1.00
	$p_{\text{true stop}}$	0.00	0.43	0.63	0.74	0.84	0.87	0.91	0.93	0.94
M4	p_{stop}	1.00	1.00	1.00	1.00	1.00	1.00	1.00	1.00	1.00
	$p_{\text{true stop}}$	0.00	0.43	0.63	0.74	0.84	0.87	0.91	0.93	0.94
M5	p_{stop}	0.00	0.00	0.35	0.40	0.47	0.55	0.62	0.69	0.76
	$p_{\text{true stop}}$	0.00	0.00	0.46	0.65	0.82	0.88	0.92	0.95	0.96
M1	p_{stop}	0.00	0.48	0.67	0.79	0.88	0.92	0.94	0.95	0.97
	$p_{\text{true stop}}$	0.00	0.38	0.70	0.80	0.87	0.90	0.93	0.95	0.96

TABLE 3: Toy example employing the properties listed in Table2. Here we are in a 10 class recursive classification scenario. To highlight the difference we set $\tau = .75$ and $\varepsilon_+ \sim \text{lognorm}(0.8, 0.5^2)$ and $\varepsilon_- \sim \text{lognorm}(-0.3, 0.5^2)$. We perform 5000 MC simulations to report each number. Here we start the recursive classification where 3 candidates share the probability weight and the remaining. Share the remainder almost uniformly. Observe that as class space expands (M3) and (M4) behave similarly. Most importantly (MP) is robust and behave similar to (M1) where the lower bound (M1) results a deficit in accuracy. (imagesrc:https://people.com/pets/tomsenn-lion-mane-dog-costume-amazon/)

Method	Number of Sequences																
	8	9	10	11	12	13	14	15	16	17	18	19	20	21	22	23	24
MP	p_{stop}	0.00	0.04	0.09	0.18	0.31	0.45	0.60	0.70	0.77	0.86	0.91	0.94	0.96	0.97	0.98	0.99
	$p_{\text{true stop}}$	0.00	0.97	0.95	0.98	0.98	0.99	0.99	0.99	1.00	1.00	1.00	1.00	1.00	1.00	1.00	1.00
M1	p_{stop}	0.00	0.01	0.05	0.11	0.21	0.33	0.48	0.60	0.70	0.81	0.91	0.94	0.96	0.97	0.98	0.99
	$p_{\text{true stop}}$	1.00	0.89	1.00	0.99	0.99	1.00	1.00	1.00	1.00	1.00	1.00	1.00	1.00	1.00	1.00	1.00
M2	p_{stop}	0.00	0.01	0.05	0.11	0.21	0.33	0.48	0.61	0.70	0.81	0.91	0.94	0.96	0.97	0.98	0.99
	$p_{\text{true stop}}$	0.00	0.90	1.00	0.99	0.99	1.00	1.00	1.00	1.00	1.00	1.00	1.00	1.00	1.00	1.00	1.00
M3	p_{stop}	0.00	0.01	0.05	0.12	0.22	0.34	0.49	0.61	0.71	0.81	0.91	0.94	0.96	0.97	0.98	0.99
	$p_{\text{true stop}}$	0.00	0.90	1.00	0.99	0.99	1.00	1.00	1.00	1.00	1.00	1.00	1.00	1.00	1.00	1.00	1.00
M4	p_{stop}	0.00	0.01	0.05	0.13	0.23	0.35	0.49	0.62	0.72	0.82	0.91	0.94	0.96	0.97	0.98	0.99
	$p_{\text{true stop}}$	0.00	0.91	0.98	0.99	0.99	1.00	1.00	1.00	1.00	1.00	1.00	1.00	1.00	1.00	1.00	1.00
M5	p_{stop}	0.00	0.00	0.00	0.00	0.00	0.00	0.00	0.01	0.03	0.08	0.13	0.18	0.23	0.28	0.33	0.38
	$p_{\text{true stop}}$	0.00	0.00	0.00	0.00	0.00	0.00	0.00	1.00	1.00	1.00	1.00	1.00	1.00	1.00	1.00	1.00
$\bar{M}1$	p_{stop}	0.01	0.04	0.10	0.20	0.33	0.47	0.61	0.72	0.79	0.88	0.94	0.96	0.97	0.98	0.99	1.00
	$p_{\text{true stop}}$	0.43	0.95	0.94	0.98	0.98	0.99	0.99	0.99	0.99	1.00	1.00	1.00	1.00	1.00	1.00	1.00

TABLE 4: Toy example employing the properties listed in Table2. Prior information in MC simulations has a fixed prior probability for the true class that is set to 0.1 and the remainder probability is distributed using a normalization to 0.9 sum value after random assignment at each simulation. We set $\tau = .85$ and $\varepsilon_+ \sim \text{lognorm}(0.8, 0.5^2)$ and $\varepsilon_- \sim \text{lognorm}(-0.3, 0.5^2)$. Observe that (MP) provides early stopping achieving the speed of ($\bar{M}1$) by losing marginal accuracy compared to (M1). Since the posterior is following a central path, uncertainty based methods and confidence methods behave similarly as explained in Sec.3.2.

These results are presented in Figure 4. On the figure left, we observe that changing decision boundaries allows us to select a sub-region from the speed-accuracy curve. In such cases (MP) provides high accuracy similar to (M1). On the figure right, where the posterior trajectory follows a central path, we observe that (MP) improves both speed and accuracy compared to other methods.

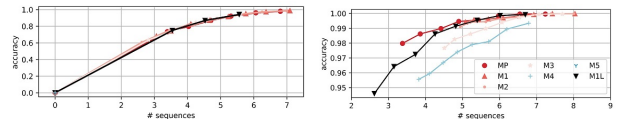


Fig. 4: Summary of operation characteristics of the methods using the starting conditions for recursive classification presented in Table3 and Table4 respectively on left and right. For our experiments we use $\varepsilon_+ \sim \text{lognorm}(0.6, 0.5^2)$ and $\varepsilon_- \sim \text{lognorm}(0, 0.5^2)$. We run 5000 recursive classification simulations and report average accuracies and average sequences for different τ values. Each line in the figure are drawn with a collection of (accuracy, sequence) points where each are computed for $\tau = [0.65, 0.69, 0.72, 0.76, 0.79, 0.83, 0.86, 0.9]$ from left to right. We omit (M5) as it spends way more sequences. Observe that (M4) staggers, especially for the disfavored case (left). (MP) allows us to select an operation point that favors accuracy in the disfavored and gains speed by losing marginal accuracy where the posterior is following a central path (right).

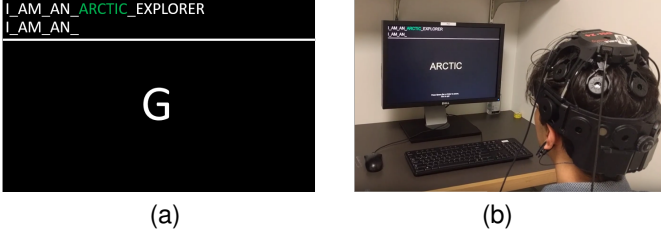


Fig. 5: EEG driven Rapid Serial Visual Presentation (RSVP) keyboard typing interface. (a) The stimuli is flashed in the middle of the screen while the user is informed with the text above. (b) The user is conducting copying the phrase task (multiple copy letter tasks). The user is informed about the required phrase. EEG is collected on top of the scalp non-invasively.

5.2 Real Data Experiments

5.2.1 Experimental Details

In our experiments we use a BCI typing system called RSVP Keyboard presented in Orhan’s work [23] and the implementation BCIPy [24]. The system is visualized for the stimulus screen and an actual healthy participant performing a task in Fig. 5.

The system visually stimulates series of letters rapidly to the user. Once intended symbol appears on the computer screen, subject’s recorded brain signal evokes a distinguishable response [25]. The system utilizes EEG to record brain signals during presentation where p300 evoked potential presence corresponds to a positive response and absence corresponds to a negative response. The user has an intended letter in mind which indicates the class label among other candidates in the alphabet. The system recursively collects noisy EEG to increase the confidence before making a decision. Subjects approximately allocate [10,30] seconds for typing a single letter and hence an increase in classification speed is of a significant value in typing sentences.

Data Collection: Ten healthy participants (six females), 20-35 years old were recruited under IRB-130107 protocol approved by Northeastern University. A DSI-24 Wearable Sensing EEG Headset was used for data acquisition, at a sampling rate of 300 Hz with active dry electrodes. All participants performed the calibration session containing 100 sequences; each sequence includes 5 trials; and one trial in each sequence is the target symbol which is displayed on the screen prior to each sequence (RSVP paradigm). A sequence contains randomly ordered ten symbols with a pre-defined target symbol. EEG is acquired from 16 channels using the International 1020 configuration (Fp1, Fp2, F3, F4, Fz, Fc1, Fc2, Cz, P1, P2, C1, C2, Cp3, Cp4, P5, P6). Recorded EEG are used to learn class conditional EEG evidence distributions.

Pre-Processing: In EEG-BCIs the primary interest of filtering is to extract the signal of interest components [26], [27]. We first filter the EEG signal to remove drifts and artifact-related high frequency components with a band pass filter for [1,50]Hz. After filtering, EEG is windowed to extract the respective evidence at each channel for stimuli presentations. Time-windowed data from different EEG channels is usually concatenated to obtain the EEG feature vector that has a high dimension because of using a multi-channel measurement.

Therefore, dimensionality reduction using ICA or PCA is also needed [26]. The system relies on reducing EEG time series into one dimensional feature vector. Filtered multi-channel EEG data time windows are passed through channel-wise principal component analysis where the outputs are concatenated to an intermediate feature vector. We assume in each class, feature vectors are drawn from a multivariate Gaussian distribution and hence Regularized discriminant analysis (regularized quadratic discriminant analysis [28]) is a plausible choice that results in one dimensional representation of the signal. Each positive and negative sample in the calibration EEG data is reduced to a single dimensional feature and positive and negative feature distributions are learned accordingly.

Experimental Task: For our experiments we use these distributions in Copy-Letter task such that each user’s data is used to type a target letter within a pre-determined phrase for multiple phrases [29]. More specifically, for each letter typing scenario the user is tasked to respond to the system, and the decision is made when the cumulative evidence matches the correct letter after multiple recursions. Therefore, in such a setting, the decision chance level is 0.03%. To make a decision the system recursively queries the user with multiple letter flashes. We designate the number of queries to be presented at each sequence to be $N \in \{15, 10, 5\}$. We present the results for two conditions. First one is a typing scenario with no language model (uniform prior information). And in the second scenario there exists a language model for the requested typing and the candidate letter is in top 16. The choice of two scenarios illustrated in the numerical results is to represent the following; (i) Class priors are uniform (in the 28-vertex simplex, RBC starts from the center of the simplex labeled as u in Figure 1-(d)). (ii) The prior probability for the correct class label (desired letter of the user) is selected to be significantly lower than in the first case (in the 28-vertex simplex, RBC starts further away from the target vertex). These cases represent typical situations with uninformative prior and adversarial prior, additionally these are the challenging cases for RBC.

5.2.2 Results

In our experiments we categorize the users based on their calibration performances. The measure of performance is the area under receiver operating characteristics curve (AUC) of classification based on the features extracted during calibration. We specifically selected user data with AUC performances $\{0.67, 0.72, 0.76, 0.81, 0.84, 0.87\}$ to have a spectrum of ranging performances.

We visualize our findings in Figure 6 and 7 respectively. It is observed that (MP) switches the operation point to a location such that faster results are obtained with the cost of small amount of decreases in accuracy. To show the significance of the (MP), we present here a scenario that includes correctly typing 100 letters on a computer screen. We refer the reader to appendix Sec. 7.3.2 for the complete results that allowed us to generate visualizations.

Comparing with the conventional method (M1), when uniform prior is used, (MP) outperforms (M1) in terms of

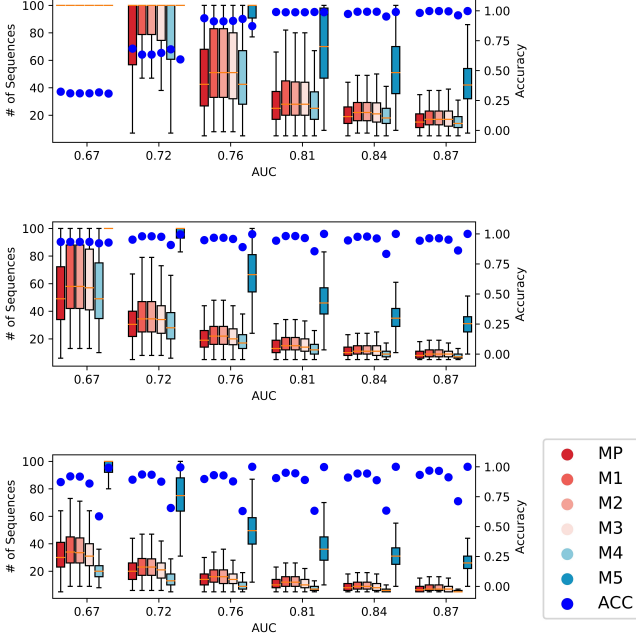


Fig. 6: Number of recursion spent and accuracy plots for recursive classification in BCI typing system. Each scenario is generated using human-in-the-loop calibration data trained generative models. In each figure results are presented in ascending order of performance measures (area under receiver operation characteristics curve (AUC)). Number of queries in each recursion from top to bottom, 5, 10, 15 respectively. Legend covers methods from left to right and dots on the figures represent respective accuracy values. The users tried to type "A" without any language model (uniform prior information). Top to bottom legend order is from left to right for each block.

speed, i.e., (MP) and (M1) complete the same task with 1735 and 1945 sequences respectively. Accordingly (MP) saves 210 sequences. This corresponds to saving $3(m)30(s)/32(m)$ lifetime during typing. Additionally, if a language model prior is used for the same task, (MP) still outperforms (M1), 1580 sequences vs 1728 sequences saving $2(m)24(s)/28(m)48(s)$ lifetime during typing. These reported amount of time are computed under the condition that at the end of the task 100 letters are completely correctly typed including corrections of the wrongly typed letters (i.e., email is completely correct). Saving time is very crucial for practical BCI typing as these systems are designed for individuals with limited speech and physical abilities. Therefore, fatigue and discomfort caused by the BCI system are important factors that significantly affect the BCI typing performance, and limiting the time to complete the tasks accurately will significantly improve practicality.

6 CONCLUSION

In this paper, our focus was on the analysis and design of stopping criterion for recursive Bayesian classification. Stopping criterion based on thresholding posterior distribution may result in redundant recursions/evidence collection. To overcome these shortcomings, uncertainty based methods were proposed. Through a geometrical representation of the posterior probability progression in a probability simplex, we demonstrated that such uncertainty methods increase the stopping region to decrease the redundancy of the posterior probability thresholding, but they are sensitive to the number

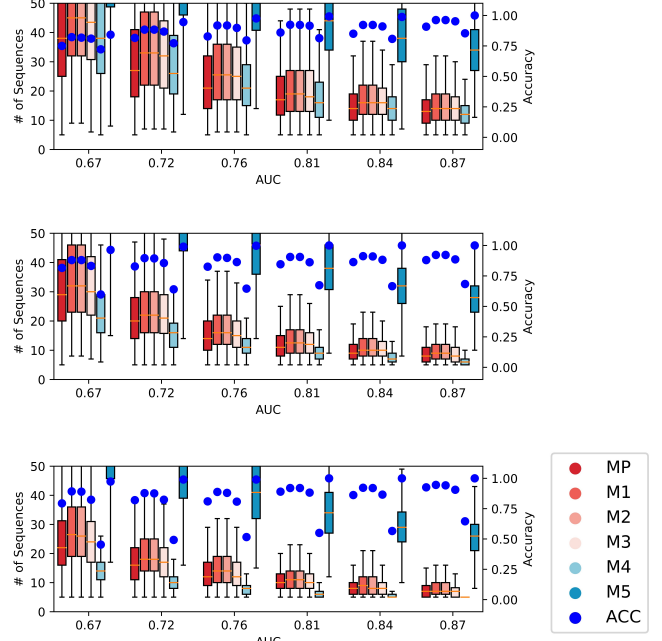


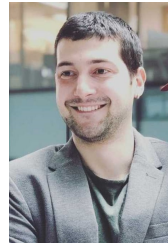
Fig. 7: The same implementation as described in Figure 6. The difference here is the subjects were supported by a language model trying to type "IT_O" given "IT_" and hence even though "O" is not the top letter it is one of the likely letters.

of classes and the increase in the stopping region is not inline with the posterior probability progression resulting in significant decrease in classification accuracy when the stopping region is enlarged. Accordingly, we proposed a new method to overcome the limitation of the existing uncertainty methods and showed that through such a method true positive probability is always larger than the true positives obtained through a stopping criterion based on thresholding posterior probability. We also showed analytically that under certain conditions true positive probability of the proposed method can be designed to be above the true positive of the method that depends on posterior thresholding while the false alarm probability of the proposed method remains within certain range. We also validated the proposed method using a real-case use on a brain computer interfaced typing system. This work can be extended by considering true positive maximization and false negative minimization as a multi-objective optimization.

REFERENCES

- [1] R. O. Duda, P. E. Hart, and D. G. Stork, *Pattern classification*. John Wiley & Sons, 2012.
- [2] H. L. Van Trees and K. L. Bell, *Detection estimation and modulation theory*. Wiley, 2013.
- [3] S. Särkkä, *Bayesian filtering and smoothing*. Cambridge University Press, 2013, vol. 3.
- [4] A. M. Alaa and M. Van Der Schaar, "Balancing suspense and surprise: Timely decision making with endogenous information acquisition," in *Advances in Neural Information Processing Systems*, 2016, pp. 2910–2918.
- [5] A. N. Shiryaev, *Optimal stopping rules*. Springer Science & Business Media, 2007, vol. 8.

- [6] S. K. Jha, E. M. Clarke, C. J. Langmead, A. Legay, A. Platzter, and P. Zuliani, "A bayesian approach to model checking biological systems," in *International Conference on Computational Methods in Systems Biology*. Springer, 2009, pp. 218–234.
- [7] I. Sason and S. Verdú, "Arimoto–rényi conditional entropy and bayesian m -ary hypothesis testing," *IEEE Transactions on Information Theory*, vol. 64, no. 1, pp. 4–25, 2017.
- [8] S. Geisser, *Predictive inference*. Routledge, 2017.
- [9] D. Golovin, A. Krause, and D. Ray, "Near-optimal bayesian active learning with noisy observations," in *Advances in Neural Information Processing Systems*, 2010, pp. 766–774.
- [10] T. L. Lai, "On optimal stopping problems in sequential hypothesis testing," *Statistica Sinica*, vol. 7, no. 1, pp. 33–51, 1997.
- [11] —, "Sequential analysis: some classical problems and new challenges," *Statistica Sinica*, pp. 303–351, 2001.
- [12] C. E. Shannon, "A mathematical theory of communication," *Bell system technical journal*, vol. 27, no. 3, pp. 379–423, 1948.
- [13] Y. Li and R. E. Turner, "Rényi divergence variational inference," in *Advances in Neural Information Processing Systems*, 2016, pp. 1073–1081.
- [14] D. Weinshall, H. Hermansky, A. Zweig, J. Luo, H. Jimison, F. Ohl, and M. Pavel, "Beyond novelty detection: Incongruent events, when general and specific classifiers disagree," in *Advances in Neural Information Processing Systems*, 2009, pp. 1745–1752.
- [15] D. S. Pavlichin and T. Weissman, "Chained kullback-leibler divergences," in *2016 IEEE International Symposium on Information Theory (ISIT)*. IEEE, 2016, pp. 580–584.
- [16] A. Banerjee, S. Merugu, I. S. Dhillon, and J. Ghosh, "Clustering with bregman divergences," *Journal of machine learning research*, vol. 6, no. Oct, pp. 1705–1749, 2005.
- [17] V. Pawlowsky-Glahn and J. J. Egozcue, "Geometric approach to statistical analysis on the simplex," *Stochastic Environmental Research and Risk Assessment*, vol. 15, no. 5, pp. 384–398, 2001.
- [18] S.-i. Amari and H. Nagaoka, *Methods of information geometry*. American Mathematical Soc., 2007, vol. 191.
- [19] J. Aitchison, "The statistical analysis of compositional data," *Journal of the Royal Statistical Society: Series B (Methodological)*, vol. 44, no. 2, pp. 139–160, 1982.
- [20] S.-W. Ho and S. Verdú, "On the interplay between conditional entropy and error probability," *IEEE Transactions on Information Theory*, vol. 56, no. 12, pp. 5930–5942, 2010.
- [21] T. Tsiligkaridis, B. M. Sadler, and A. O. Hero, "Collaborative 20 questions for target localization," *IEEE Transactions on Information Theory*, vol. 60, no. 4, pp. 2233–2252, 2014.
- [22] J. Kittler and C. Zor, "Delta divergence: A novel decision cognizant measure of classifier incongruence," *IEEE transactions on cybernetics*, vol. 49, no. 6, pp. 2331–2343, 2018.
- [23] U. Orhan, K. E. Hild, D. Erdogmus, B. Roark, B. Oken, and M. Fried-Oken, "Rsvp keyboard: An eeg based typing interface," in *2012 IEEE International Conference on Acoustics, Speech and Signal Processing (ICASSP)*. IEEE, 2012, pp. 645–648.
- [24] T. Memmott, A. Koçanaoğulları, M. Lawhead, D. Klee, S. Dudy, M. Fried-Oken, and B. Oken, "Bcipy: Brain-computer interface software in python," *arXiv preprint arXiv:2002.06642*, 2020.
- [25] G. F. Woodman, "A brief introduction to the use of event-related potentials in studies of perception and attention," *Attention, Perception, & Psychophysics*, vol. 72, no. 8, pp. 2031–2046, 2010.
- [26] M. Akcakaya, B. Peters, M. Moghadamfalahi, A. Mooney, U. Orhan, B. Oken, D. Erdogmus, and M. Fried-Oken, "Noninvasive brain computer interfaces for augmentative and alternative communication," *IEEE Reviews in Biomedical Engineering*, vol. 7, no. 1, pp. 31–49, 2014.
- [27] M. Moghadamfalahi, U. Orhan, M. Akcakaya, H. Nezamfar, M. Fried-Oken, and D. Erdogmus, "Language-model assisted brain computer interface for typing: A comparison of matrix and rapid serial visual presentation," *IEEE Transactions on Neural Systems and Rehabilitation Engineering*, vol. 23, no. 5, pp. 910–920, 2015.
- [28] J. H. Friedman, "Regularized discriminant analysis," *Journal of the American statistical association*, vol. 84, no. 405, pp. 165–175, 1989.
- [29] U. Orhan, H. Nezamfar, M. Akcakaya, D. Erdogmus, M. Higger, M. Moghadamfalahi, A. Fowler, B. Roark, B. Oken, and M. Fried-Oken, "Probabilistic simulation framework for eeg-based bci design," *Brain-Computer Interfaces*, vol. 3, no. 4, pp. 171–185, 2016.
- [30] C. Barceló-Vidal, J. A. Martín-Fernández, and V. Pawlowsky-Glahn, "Mathematical foundations of compositional data analysis," in *Proceedings of IAMG*, vol. 1, 2001, pp. 1–20.
- [31] A. Rényi *et al.*, "On measures of entropy and information," in *Proceedings of the Fourth Berkeley Symposium on Mathematical Statistics and Probability, Volume 1: Contributions to the Theory of Statistics*. The Regents of the University of California, 1961.



Aziz Koçanaoğulları received the B.S. degree in electrical and computer engineering and mathematics from Istanbul Technical University, Istanbul Turkey in 2014 and 2015 respectively. He received M.Sc. degree in Telecommunications Engineering in Istanbul Technical University in 2016. Since then, he has been with the Cognitive Systems Laboratory (CSL) at Northeastern University Boston, MA, USA where he is currently a Ph.D. degree candidate. His main areas of research interest are active recursive inference in sequential decision making processes and active model learning.



Murat Akcakaya received the Ph.D. degree in electrical engineering from Washington University in St. Louis, MO, USA, in December 2010. He is an Assistant Professor in the Electrical and Computer Engineering Department of the University of Pittsburgh. His research interests are in the areas of statistical signal processing and machine learning.



Deniz Erdoğan received the B.S. degree in electrical engineering and mathematics, and the M.S. degree in electrical engineering from the Middle East Technical University, Ankara, Turkey, in 1997 and 1999, respectively, and the Ph.D. degree in electrical and computer engineering, in 2002, from the University of Florida, Gainesville, FL, USA, where he was a postdoc until 2004. He is currently a Research Professor at Northeastern University. His research focuses on statistical signal processing and machine learning with applications to biomedical signal/image processing and cyberhuman systems.

7 APPENDIX

7.1 How algebra works in posterior updates

Addition: Given $p, q \in \Delta_n$

$$p \oplus q = \frac{[p_1 q_1, p_2 q_2, \dots, p_n q_n]}{\sum_i p_i q_i}$$

Given $p(\sigma) \in \Delta_{|\mathcal{A}|}$ where \mathcal{A} is the state space and $p(\varepsilon|\sigma, \phi) = [p(\varepsilon|\sigma_1, \phi), p(\varepsilon|\sigma_2, \phi), \dots, p(\varepsilon|\sigma_{|\mathcal{A}|}, \phi)]$; $p(\varepsilon|\sigma_{|\mathcal{A}|}, \phi) \notin \Delta_{|\mathcal{A}|}$ and hence one cannot rigorously define $p(\sigma) \oplus p(\varepsilon|\sigma, \phi)$. To be able to do such $p(\varepsilon|\sigma, \phi)$ should be unit ℓ_1 norm wrt. σ and hence we require $p(\varepsilon|\sigma, \phi) / (\sum_{\sigma} p(\varepsilon|\sigma, \phi))$ which is not practical. However the closure operator (normalization as defined in [19]) that maps an arbitrary point to Δ_n allows algebraically $p(\sigma) \oplus p(\varepsilon|\sigma, \phi)$ as the following;

$$\begin{aligned} p(\sigma) \oplus \frac{p(\varepsilon|\sigma, \phi)}{\sum_{\sigma} p(\varepsilon|\sigma, \phi)} &= \frac{[p(\sigma_i) p(\varepsilon|\sigma_i, \phi)]_i / \sum_{\sigma} p(\varepsilon|\sigma, \phi)}{\sum_i (p(\sigma_i) p(\varepsilon|\sigma_i, \phi)) / \sum_{\sigma} p(\varepsilon|\sigma, \phi)} \\ &= \frac{[p(\sigma_i) p(\varepsilon|\sigma_i, \phi)]_i}{\sum_i (p(\sigma_i) p(\varepsilon|\sigma_i, \phi))} \simeq p(\sigma) \oplus p(\varepsilon|\sigma, \phi) \end{aligned}$$

Following this equation we represent a posterior with the following update; $p(\sigma|\varepsilon, \phi) = p(\sigma) \oplus p(\varepsilon|\sigma, \phi)$ which is analogous with posterior=prior \oplus likelihood.

7.2 Uncertainty Decision Boundaries / The reason behind analytically analyzing only (M3)

In this section we reason the decision on only analyzing Shannon's entropy in Section 3.1. In information theory, Renyi entropy generalizes Shannon entropy [31]. The definition for Renyi entropy, parameterized over α is the following;

$$p \in \Delta_n, H_{\alpha}(p) = \frac{1}{1-\alpha} \log \sum_i p_i^{\alpha} \quad (7)$$

Observe that the limit case $\lim_{\alpha \rightarrow 1} H_{\alpha}(p) = H(p)$ results in Shannon entropy measure. In this paper we only propose analytical derivations for Shannon entropy as a special case. However the findings can directly be applied to Renyi measures. The generalization can be analytically shown, but to have a neat presentation we omit the derivations here. However, in Fig.8 we present decision boundaries for Renyi entropy and Shannon as a special case to demonstrate their similar decision geometry.

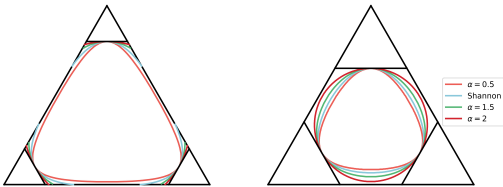


Fig. 8: Decision boundaries formed using \mathcal{S}_O for Renyi using $\alpha \in \{2, 1.5, 0.5\}$ and Shannon entropy (2, 1.5, Shannon, 0.5 in the outer to inner order in the figures). Confidence lines are plotted for reference. Corresponding values for confidence lines are $\tau = 0.8$ for left and $\tau = 0.65$ for right figure.

7.3 Proposed Method Supplementary

7.3.1 True Positive - False Alarm Guarantee

In this section we present true selection and error probabilities for simple examples that can be visualized on a three class simplex Δ_3 . We present these results to support our claims in Section 4 of the manuscript. We pick several points on the simplex and with a predefined evidence distribution sampling from a lognormal, we visualize the bounds on error in Figure 9 below. We plot the analytical bounds derived in the proof of Proposition 5 using lognormal distribution assumptions. Lower bound is represented with (M1)(red) and the upper bound is represented with (M1) (black). Instead of plotting the analytic values of (MP) we plot the average probability values calculated over 5000 Monte Carlo simulations. We compute $p(p_s \in S_R)$ and $p(p_s \in S'_R)$ values for different starting points that are color coded in the figure. To generate the figures we use $\varepsilon = [\varepsilon_+, 1, \dots, 1]$ where $\varepsilon_+ \sim \text{lognorm}(0.8, 0.6^2)$ and the true class is a . Given this evidence model, all posteriors follow a straight path to corner a (this behavior is discussed in Lemma 1 in the manuscript).

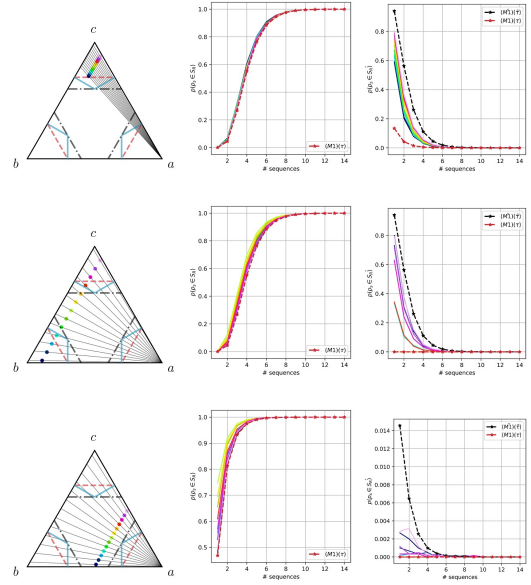


Fig. 9: In this figure we compare the probability of correct selection (reaching the correct stopping region) by # of sequences and incorrect selection in Δ_3 of (MP) (blue) with (M1) (red) and (M1) (black). 1st column represents the prior points of the recursive classification with different colors in Δ_3 . 2nd column represents the probability of posterior at sequence s lying on the correct region for stopping. 3rd column represents the probability of incorrect stopping by sequences. Observe that as described in Proposition 5 probability of correct decision is always above (M1) and probability of error is sandwiched with lower (M1) and upper (M1) curves.

In this paper we do not provide a complete analysis on the effects of the evidence distribution. However, by nature, in recursive Bayesian classification tasks, the separation of the evidence from different classes increases both accuracy and speed. We pick the prior points demonstrated in Figure 9 and investigate the effects of the distribution on probability of reaching the correct region and probability of reaching an incorrect region. For our experiments, we assume the system only collects evidence from an assumed distribution $\varepsilon = [\varepsilon_+, 1, \dots, 1]$ where $\varepsilon_+ \sim \text{lognorm}(\mu, c^2)$ for $s = 5$

times. We visualize our findings for a range of parameters in Figure 10. As expected, as we increase the standard deviation (c) of the exponentiated Gaussian distribution, the system is more likely to make errors and less likely to decide correctly. On the other hand as mean (μ) increases, the system yields more accurate decisions and less error.

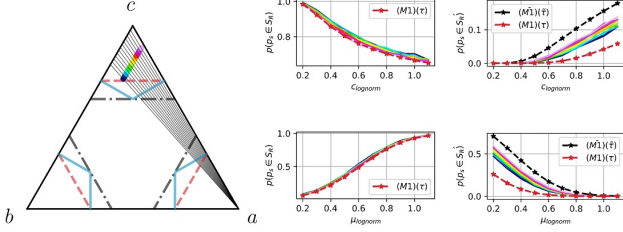


Fig. 10: In this figure we visualize the effects of the distribution variance and mean in recursive classification for the represented points in the figure. We consider $\varepsilon_+ \sim \text{lognorm}(\mu, c^2)$ and calculate the probabilities for a set sequence number $s = 5$. We represent 4 figures to indicate the effects (on the right side of the Δ_3 simplex with corners a , b and c). Top row represents the effects of the standard deviation of the exponentiated Gaussian distribution on probability of correct selection and incorrect selection for left and right respectively where $\mu = 0.8$. Whereas bottom row visualizes the effects of the mean where $c = 0.6$. It is observed as mean increases (since the evidence gets higher values) probability of correct selection increases where error chance decreases. On the other hand results are the opposite as expected for the standard deviation increments.

Through the Figures 9 and 10, we summarize our claims that are presented in Section 4 especially about the bounds on error and correct selection probability given in Proposition 5.

7.3.2 BCI Typing Supplementary

In experiments section (Sec.5), we report time required for a subject to successfully complete a 100 letter typing scenario only for the conventional method (M1). We use the following computation to report required number of sequences to complete the task;

```

acc, seq from user data; rem = 100, #seq = 0
while rem > 0 do:
    rem ← rem − ceil(rem × acc/100)
    #seq ← #seq + rem × seq
end
return #seq

```

In Table 5 we report the performance values for all the methods that are compared to (MP). We specifically report the number sequences required for each user to successfully complete the task in addition to the number of sequences averaged across all participants. Moreover, we report average typing accuracy and sequence required to type 1 letter (correct or incorrect) for each method averaged across users. It is apparent (MP) allows faster typing as reported in the experiments by an accuracy loss of 5% on average. (M4) seems to outperform (MP) in the uniform case. However, (M4) results in frequent incorrect decisions that require corrections which irritates the target population to use such BCI systems. Therefore, such methods similar to (M4) may overall perform worse due to fatigue effects.

LM	Perf	Seq	Sequence Difference from # (MP)				
		# (MP)	(M1)	(M2)	(M3)	(M4)	(M5)
Uniform	67	3628	+327	+306	+143	-183	+5687
	72	2290	+295	+279	+142	-130	+5200
	76	1627	+197	+186	+85	-59	+3391
	81	1180	+186	+173	+93	+18	+2524
	84	947	+129	+124	+677	+14	+2173
	87	739	+126	+122	+71	+35	+1921
	avg	1735	+210	+198	+101	-50	+3482
Language Model	acc	90%	94%	94%	88%	64%	99%
	E(seq)	15.44	18.07	17.96	16.05	10.70	51.95
	67	3012	+194	+202	+11	+110	+3252
	72	2053	+233	+224	+78	+21	+3208
	76	1570	+147	+141	+62	-43	+2743
	81	1171	+119	+115	+43	-22	+2276
	84	923	+104	+105	+51	+43	+2018
	87	754	+95	+89	+49	+58	+1865
	avg	1580	+148	+146	+490	+27	+2560
	acc	85%	90%	90%	85%	56%	98%
	E(seq)	13.08	15.68	15.57	13.90	8.46	41.04

TABLE 5: Supplementary for BCI experiments Fig.6, Fig.7. For all experiments the confidence threshold is set to $\tau = .85$ for (M1) and the constants for the other objectives are calculated accordingly. We report number of sequences spent for (MP) for different performing users and corresponding differences with other methods. *avg* represents the average sequence values for each method conditioned on LM respectively. *acc* and *E(seq)* represent accuracy in typing and average number of sequences spent for 1 letter respectively. For the language model case, based on prior location for "O" after "IT_", the difference between (M4) vanishes.

7.4 Proofs

Proof Proposition 1. Addition: Given $p, q \in \Delta_n$ the addition operation is defined as the following;

$$p \oplus q = \frac{[p_1 q_1, p_2 q_2, \dots, p_n q_n]}{\sum_i p_i q_i}$$

Multiplication with scalar: Given $p \in \Delta_n, \lambda \in \mathbb{R}$ the multiplication with scalar is defined as the following;

$$p \otimes \lambda = \frac{[p_1^\lambda, p_2^\lambda, \dots, p_n^\lambda]}{\sum_i p_i^\lambda}$$

Let $p, q, r \in \Delta_n; p \oplus q = [(p \oplus q)_k | k \in \{1, 2, \dots, n\}] \in \mathbb{R}^n$ and $p \otimes q = [(p \otimes q)_k | k \in \{1, 2, \dots, n\}] \in \mathbb{R}^n$

Additive Closure: $p_k > 0, q_k > 0 \implies [p \oplus q]_k > 0, \sum_k [p \oplus q]_k = \sum_k p_k q_k / \sum_i p_i q_i = 1 \implies p \oplus q \in \Delta_n$

Scalar Closure: $p_k > 0, \lambda \in \mathbb{R} \implies p_k^\lambda > 0 \implies [p \otimes \lambda]_k > 0, \sum_k [p \otimes \lambda]_k = \sum_k p_k^\lambda / \sum_i p_i^\lambda = 1 \implies p \otimes \lambda \in \Delta_n$

Commutativity: scalar multiplication is commutative $\implies p_k q_k = q_k p_k \implies p \otimes q = q \otimes p$

Additive Associativity: scalar multiplication is associative $\implies (p_k q_k) r_k = p_k (q_k r_k) \cdot [p \oplus q]_i = p_i q_i / \sum_k p_k q_k, [(p \oplus q) \oplus r]_i = p_i q_i r_i / \sum_k p_k q_k r_k \implies (p \oplus q) \oplus r = p \oplus (q \oplus r)$

Zero Element: $u_n \in \Delta_n$ as shown above.

Multiplicative 1: $[p \otimes 1]_k = p_k / \sum_i p_k = p_k \implies p \otimes 1 = p$

The following properties can be shown using the definitions above easily and hence omitted; additive inverses, scalar multiplication associativity, distributivity across vector addition, distributivity across scalar addition. \square

Proof Proposition 2. $S_\tau = \{p | \max_i p_i = \tau\} \implies \max_{p \in S_\tau} H(p) = H(v_n(\tau))$

Let $p \in S_\tau$. WLOG pick $p_1 = \tau$ where $|p| = n$;

$$\begin{aligned} \max_p H(p) &= \max_{p_i \in p} -p_1 \log(p_1) - \sum_{i \in \{2, \dots, n\}} p_i \log(p_i) \\ &\quad \text{from principle of maximum entropy} \\ &= -\tau \log(\tau) - \sum_{i \in \{2, \dots, n\}} \frac{1-\tau}{n-1} \log\left(\frac{1-\tau}{n-1}\right) \\ &= -\tau \log(\tau) - (1-\tau) \log\left(\frac{1-\tau}{n-1}\right) \\ &= H(v_n(\tau)) \end{aligned}$$

$$S_\tau = \{p | H(p) = H(v_n(\tau))\} \implies \max_{i, p \in C_\tau} p_i = \tau$$

Let $p \in C_\tau$. WLOG pick $i = 1, p \in C_\tau \implies p_1 \log p_1 = -H(v_n(\tau)) - \sum_{i \in \{2, \dots, n\}} p_i \log p_i$

$$\begin{aligned} &\left. \frac{d x \log(x)}{dx} \right|_{x \in (1/e, \infty)} > 0 \\ \implies \max_x x &= \arg \max_x x \log(x) \quad \forall x \in (1/e, \infty) \\ \implies \max_{p \in C_\tau} p_1 &= \arg_{p_1} \max_{p \in C_\tau} p_1 \log p_1 \\ &= \arg_{p_1} \max_{p \in C_\tau} -H(v_n(\tau)) - \sum_{i \in \{2, \dots, n\}} p_i \log p_i \\ &= \arg_{p_1} \max_{p \in C_\tau} - \sum_{i \in \{2, \dots, n\}} p_i \log p_i \\ &\quad \text{where } \sum_{i \in \{2, \dots, n\}} p_i = 1 - p_1 \end{aligned}$$

Using the identity $\hat{x} = \arg \max_x -\log(x)^T x = [1/e, \dots, 1/e]^T$ then project to $(1 - p_1)$ -unit ℓ_1 norm ball again from principle of maximum entropy we observe $p_{1:n} = [\frac{1-p_1}{n-1}, \dots, \frac{1-p_1}{n-1}] \implies p = [p_1, \frac{1-p_1}{n-1}, \dots, \frac{1-p_1}{n-1}] = v_n(p_1)$. Since $H(p) = H(v_n(p_1)) = H(v_n(\tau))$, $p_1 = \tau$. \square

Proof Observation 1. Derivation is trivial given Proposition 2. Omitted. \square

Proof Observation 2. Let $p \in \Delta_n$, WLOG $p_1 = \max_i p_i$;

$$\begin{aligned} H(p) &= -\sum_i p_i \log(p_i) = -p_1 \log(p_1) - \sum_{i \in \{2, \dots, n\}} p_i \log(p_i) \\ &\leq -p_1 \log(p_1) - (1 - p_1) \log\left(\frac{1 - p_1}{n - 1}\right) \quad (8) \\ -H(p) &\geq p_1 \log(p_1) + (1 - p_1) \log\left(\frac{1 - p_1}{n - 1}\right) \end{aligned}$$

Let $f(u, a) = u \log(u) + (1 - u) \log\left(\frac{1 - u}{a - 1}\right)$ for $u \in [1/a, 1]$ and $a \geq 1$; $f(u, a)$ is strictly convex and monotonically increasing for $\forall u \in [1/a, 1]$ where $a \geq 1$. If $p_1 \geq \tau$ then $f(p_1, n) \geq f(\tau, n)$. This concludes that;

$$-H(p) \geq \tau \log(\tau) + (1 - \tau) \log\left(\frac{1 - \tau}{n - 1}\right) = -\tau' \quad (9)$$

Therefore, $\forall p_1 \geq \tau \geq 1/n \implies H(p) \leq \tau'$. Hence $\forall p \in S_1 \implies p \in S_2$ which concludes $S_1 \subseteq S_2$.

Moreover, given $n = 5$ where $\tau' = 2.16$, therefore corresponding $\tau = 0.5$. Pick a distribution with probabilities $p = \{.4, .2, .2, 0, 0\}$. Obviously, $p \notin S_1$. However, $H(p) = 1.5219 < \tau'$ therefore $p \in S_2$ which shows $S_2 \not\subseteq S_1$. Bu the counterexample $S_1 \subseteq S_2$ reduces to $S_1 \subset S_2$. \square

Proof Observation 3. The edge case for equi-entropy contours intersecting with the edges of the probability domain is WLOG $p = [0.5, 0.5, 0, \dots, 0]$ hence $H(p) = 1$. $H(v_n(\tau)) < 1 \implies$ the equi entropy contour S_τ intersects with the borders of the simplex. As explained over truncated distributions in [20], we use the confidence line definition $C_\tau = \{p | \max_i p_i = \tau\}$ and use the identity $\arg \max_{p \in C_\tau} H(p) = w_n(\tau)$. Equivalently, for $w_n(\tilde{\tau})$ to hold the entropy condition, one can write;

$$-\tilde{\tau} \log_2(\tilde{\tau}) - (1 - \tilde{\tau}) \log_2(1 - \tilde{\tau}) = H(v_n(\tau))$$

\square

Proof Lemma 1. Pick $a_1, a_2, a_n \in \mathcal{A}$ being 1st, 2nd, n^{th} class respectively and a_1 being queried $\phi(a_1)$ with initial probability distribution over the entire state space $p(\sigma) = [p_{a_1} = p_1, \dots, p_n]$ yielding the evidence ε . Observe the following relation between the posterior and prior using the label assignment for the queried candidate ℓ where for a query $\phi(a_c)$, and a candidate $a_{c'}, a_{c'} = a_c \implies \ell = 1$;

$$\begin{aligned} p(\sigma | \varepsilon, \phi(a_1)) &= p(\sigma) \oplus p(\varepsilon | \sigma, \phi(a_1)) \\ &= p(\sigma) \oplus [p(\varepsilon | a_1, \phi(a_1)), p(\varepsilon | a_2, \phi(a_1)), \dots, p(\varepsilon | a_n, \phi(a_1))] \\ &= [p(\varepsilon | \ell = 1), p(\varepsilon | \ell = 0, \dots, p(\varepsilon | \ell = 0))] \end{aligned}$$

The following vectors map to the same point on simplex; $[p(\varepsilon | \ell = 1), p(\varepsilon | \ell = 0), \dots, p(\varepsilon | \ell = 0)] \sim [\frac{p(\varepsilon | \ell = 1)}{p(\varepsilon | \ell = 0)}, 1, \dots, 1]$

$$\begin{aligned} p(\sigma | \varepsilon, \phi(a)) &= p(\sigma) \oplus p(\varepsilon | \sigma, \phi(a)) \\ &= p(\sigma) \oplus \left[\frac{p(\varepsilon | \ell = 1)}{p(\varepsilon | \ell = 0)}, 1, \dots, 1 \right] \\ &= p(\sigma) \oplus [k, 1, \dots, 1] \text{ where } k = \frac{p(\varepsilon | \ell = 1)}{p(\varepsilon | \ell = 0)} \in \mathbb{R}^+ \\ &\quad \propto [p_1 \times k, p_2, \dots, p_n] \end{aligned}$$

First we write the posterior using the previous equation;

$$\begin{aligned} p(\sigma | \varepsilon, \phi(a_1)) &= \left[\frac{p_1 \times k}{m}, \frac{p_2}{m}, \dots, \frac{p_n}{m} \right] \in \Delta_N \\ &\quad \text{where } m = p_1 \times (k - 1) + 1 \end{aligned}$$

Trivially, $p(\sigma)$ and $[1, 0, \dots]$ form a line. To show collinearity, we show $p(\sigma | \varepsilon, \phi(a_1))$ also lies on that line, in other the point should satisfy the line equation;

$$(\text{line}) : \frac{x_1 - 1}{p_1 - 1} = \frac{x_2}{p_2} = \dots = \frac{x_n}{p_n}$$

If we insert $x_1 = p_1 \times k/m$ and respective remaining probabilities;

$$\frac{((p_1 \times k)/m) - 1}{p_1 - 1} \stackrel{?}{=} \frac{p_2/m}{p_2} = \dots = \frac{p_n/m}{p_n} = \frac{1}{m}$$

We show collinearity with the following algebraic manipulation;

$$\begin{aligned} m = p_1(k-1) + 1 &\implies \frac{((p_1 \times k)/m) - 1}{p_1 - 1} \\ &= \frac{p_1 \times k - p_1 \times k + p_1 - 1}{(p_1 - 1) \times m} = \frac{1}{m} \end{aligned}$$

□

Proof Lemma 2. Given $p(\sigma) = [p(a), p(b), \dots, p(z)] \in \Delta_n$ and WLOG for element $i = 1$ denoting the special position the line $\ell_{c_n, i=1} = \{[\tau, \frac{1-\tau}{n-1}, \dots, \frac{1-\tau}{n-1}] | \forall \tau \in [0, 1]\}$. Observe that $\ell_{c_n, i=1}$ only includes $v_n(\cdot)$ special distributions and hence we can rewrite the minimization as the following;

$$\text{proj}_{\ell_{c_n, i=1}}(p(\sigma)) = \arg \min_{\tau} \|p(\sigma) - w_n(\tau)\|_2^2$$

Equating the first derivative to 0;

$$\begin{aligned} \frac{\delta}{\delta \tau} \|p(\sigma) - v_n(\tau)\|_2^2 &= m^T p(\sigma) - m^T w_n(\tau) = 0 \\ \text{where } m &= [1, \frac{-1}{n-1}, \dots, \frac{-1}{n-1}] \end{aligned}$$

Calculating on an element basis;

$$\begin{aligned} p(a) - \frac{p(b)}{n-1} - \dots - \frac{p(z)}{n-1} &= \tau + \frac{\tau-1}{(n-1)^2}(n-1) \\ p(a) - \frac{1-p(a)}{n-1} &= \tau + \frac{\tau-1}{(n-1)} \implies p(a) = \tau \end{aligned}$$

Therefore,

$$\text{proj}_{\ell_{c_n, i=1}}(p(\sigma)) = v_n(p(a)) = [p(a), \frac{1-p(a)}{n-1}, \dots, \frac{1-p(a)}{n-1}]$$

This proof can be extended to any distance metric defined over simplex following Barcelo's work [30] Section 3-4. The only requirement is to define invertible centering transform H_D and using centering log-ratio transform. With these transforms one can find an approximate mapping between the simplex and ℓ_2 and hence solve $\arg \min_{\tau} \|H_{D\text{clr}}(p(\sigma)) - H_{D\text{clr}}(w_n(\tau))\|_2^2$, the approximate solution is the same. □

Proof Proposition 3. Given $p(\sigma) = [p(a), p(b), \dots, p(z)]$ and from Lemma 2 $\text{proj}_{\ell_{c_n, i=1}} p(\sigma) = w_n(p(a))$. Hence;

$$\begin{aligned} &\|p(\sigma) - w_n(p(a))\|_2^2 \\ &= \left\| \left[0, p(b) - \frac{1-p(a)}{n-1}, \dots, p(z) - \frac{1-p(a)}{n-1} \right] \right\|_2^2 \\ &= \sum_{c \in A \setminus \{a\}} \left(p(c) - \frac{1-p(a)}{n-1} \right)^2 \leq \left(1 - p(a) - \frac{1-p(a)}{n-1} \right)^2 \\ &= (1-p(a))^2 \frac{(n-2)^2}{(n-1)^2} \propto (1-p(a))^2 \end{aligned}$$

In Lemma 1, following the assumption $p(\sigma | \mathcal{H}_s)$ increases on average, using the averaged evidence for each state, query (σ, ϕ) brings posterior towards $\ell_{c_n, i}$ closer each s . □

Observation 6.

$$\begin{aligned} p, q \in \Delta_n, j_1 &= \arg \max_i p_i, j_2 = \arg \max_{i \neq j_1} p_i \\ k_1 &= \arg \max_i q_i, k_2 = \arg \max_{i \neq k_1} q_i, \\ I &= \{j_1, j_2, k_1, k_2\}, p' = 1 - \sum_{i \notin I} p_i, q' = 1 - \sum_{i \notin I} q_i \\ \delta_{\text{delta}^2}(p, q) &= \frac{1}{2} \left[\sum_{i \in I} |p_i - q_i| + |p' - q'| \right] \end{aligned}$$

$\bigcup_{k \in \{1, 2, \dots, n\}} \tilde{B}_{\delta}^{\bar{\tau}}(c^k)$ with $\delta = \delta_{\text{delta}^2}$ yields confidence thresholding.

Proof. Observation 6

WLOG 1st location is the point of interest, hence the respective boundary includes probabilities with 1st element being the maximum valued; $q, p \in \Delta_n$ where $q = [1, 0, \dots, 0]$ and $p = [p_1, p_2, \dots, p_n]$ with $1 = \arg \max_i p_i$. Observe that;

$$\begin{aligned} j_1 &= \arg \max_i p_i = 1 \quad j_2 = \arg \max_{i \neq 1} p_i \\ k_1 &= \arg \max_i q_i = 1 \quad k_2 = \arg \max_{i \neq 1} q_i = \hat{i}, \forall \hat{i} \in 2, 3, \dots, n \end{aligned}$$

WLOG pick $k_2 = j_2$. Hence $I = \{1, j_2\} \implies p' = 1 - p_{j_1} - p_{j_2}, q' = 0$. Inserting these into the following delta divergence equation;

$$\begin{aligned} \delta_{\text{delta}^2}(p, q) &= \frac{1}{2} \left[\sum_{i \in I} |p_i - q_i| + |p' - q'| \right] \\ &= \frac{1}{2} (1 - p_1 + p_2 + 1 - p_1 - p_2) = 1 - p_1 \end{aligned}$$

Hence the decision condition $\delta_{\text{delta}^2}(p, q) < \bar{\tau} \implies p_{j_1} > 1 - \bar{\tau} \implies \max_i p_i > 1 - \bar{\tau}$. Confidence thresholding and delta divergence are equivalent. □

Proof Proposition 4. Following Obs.6;

WLOG 1st location is the point of interest, hence the respective boundary includes probabilities with 1st element being the maximum valued; $q, p \in \Delta_n$ where $q = [1, 0, \dots, 0]$ and $p = [p_1, p_2, \dots, p_n]$ with $1 = \arg \max_i p_i$. Observe that;

$$\begin{aligned} j_1 &= \arg \max_i p_i = 1 \quad j_2 = \arg \max_{i \neq 1} p_i \\ k_1 &= \arg \max_i q_i = 1 \quad k_2 = \arg \max_{i \neq 1} q_i = \hat{i}, \forall \hat{i} \in 2, 3, \dots, n \end{aligned}$$

WLOG pick $k_2 = j_2$. Hence $I = \{1, j_2\} \implies p' = 1 - p_{j_1} - p_{j_2}, q' = 0$. Inserting these into the following modified delta divergence equation;

$$\delta_{\text{MP}}(p, q) = \left[\sum_{i \in I} |p_i - q_i| \right] = 1 - p_{j_1} + p_{j_2}$$

Following the decision condition $\delta_{\text{MP}}(p, q) < \bar{\tau} \implies 1 - p_{j_1} + p_{j_2} < \bar{\tau} \implies p_{j_1} - p_{j_2} > 1 - \bar{\tau}$.

Therefore using the ball definition for $\delta = \delta_{MP}$ and $q = [1, 0, \dots, 0]$ $\tilde{B}_\delta^\tau(q) = \{x | \delta(q, x) < \bar{\tau}, x \in \Delta_n\} \implies$

$$\tilde{B}_\delta^\tau(a) = \{x | x_j - x_k > 1 - \bar{\tau}, j = \arg \max_i x_i, k = \arg \max_{i \neq j} x_i, x \in \Delta_n\}$$

□

Proof Observation 4. Define the following two sets;

$$C_\tau = \{p | \arg \max_i p_i = 1, \max_i p_i = \tau\}$$

$$B_{\bar{\tau}} = \left\{ p | p_1 - p_m = 1 - \bar{\tau}, 1 = \arg \max_i p_i, m = \arg \max_{i \neq 1} p_i \right\}$$

Observe, $\max_{p \in B_{\bar{\tau}}} p_i = p_1$. We seek the following;

$$\max_{p \in B_{\bar{\tau}}} p_1 \text{ s.t. } 1 = \arg \max_i p_i$$

$$\implies \max_{p \in B_{\bar{\tau}}} 1 - \bar{\tau} + p_m \text{ s.t. } 1 = \arg \max_i p_i, m = \arg \max_{i \neq 1} p_i$$

$$\implies \max_{p \in B_{\bar{\tau}}} p_m \text{ s.t. } 1 = \arg \max_i p_i, m = \arg \max_{i \neq 1} p_i$$

Trivially, $\max p_m = 1 - p_1 \implies p_1 = 1 - \bar{\tau} + 1 - p_1 \rightarrow p_1 = 1 - \bar{\tau}/2$. Observe that $p_i = 0 \forall i \neq \{1, m\}$ and hence $p = w_n(1 - \bar{\tau}/2)$. If $\bar{\tau} = 2\tau - 2$ then $p = w_n(\tau)$ and $\arg \max_{p \in B_{2-2\tau}} p_1 = w_n(\tau)$.

Observe $w_n(\tau) \in C_\tau$, $w_n(\tau) \in B_{2-2\tau}$ and by the equality condition in both sets, $w_n(\tau) = (C_\tau \cap B_{2-2\tau})$. □

Proof Observation 5. Define the following;

$$B_{\bar{\tau}} = \left\{ p | p_1 - p_m = 1 - \bar{\tau}, 1 = \arg \max_i p_i, m = \arg \max_{i \neq 1} p_i \right\}$$

By definition, $\min_{p \in B_{\bar{\tau}}} p_i = p_1 \cdot p \in B_{\bar{\tau}} \implies p_1 - p_m = 1 - \bar{\tau}$. Following a similar procedure as described in proof for Observation 4. $\arg \min_p p_1 \sim \arg \min_p 1 - \bar{\tau} + p_m$, hence we seek to minimize p_m such that $m = \arg \max_{i \neq 1} p_i$. p_m is trivially minimized by setting $p_m = (1 - p_1)/(n - 1)$ hence resulting in $p = v_n(p_1)$.

Observe that $p_1 - p_m = 1 - \bar{\tau} = p_1 - (1 - p_1)/(n - 1) \implies p_1 = (1 + \bar{\tau}(n - 1))/n$. □

Lemma 3. $p(\sigma|\varepsilon_{0:s}) \in \Delta_n \forall s \in \{0, 1, \dots\}$ with $p(\sigma|\varepsilon_{0:s}) = p(\sigma) \oplus p(\varepsilon_0|\sigma) \oplus \dots \oplus p(\varepsilon_s|\sigma)$, and \mathcal{R}_S denotes the stopping region s.t. $(S) : p(\sigma|\varepsilon_{0:s}) \in \mathcal{R}_S$. WLOG, let 1^{th} location belong to the target class. Given $p(\varepsilon_s|\sigma) \propto [\varepsilon, 1, \dots, 1]$ then the following relations hold;

$$(1) S_{R(M1)} = \{p | p_1 \geq \tau, p \in \Delta_n\}$$

$$\implies \arg \min_s (p(\sigma|\varepsilon_{0:s}) \in \mathcal{R}_S) = \hat{s} > \log_\varepsilon \frac{(1 - p_1)\tau}{(1 - \tau)p_1}$$

$$(2) S_{R(MP)} = \left\{ p | p_1 - p_i \geq \tau_{(2)}, i = \arg \max_{i \neq 1} p_i, p \in \Delta_n \right\}$$

$$\implies \arg \min_s (p(\sigma|\varepsilon_{0:s}) \in \mathcal{R}_S) = \hat{s} > \log_\varepsilon \frac{(1 - p_1)\tau_{(2)} + p_i}{(1 - \tau_{(2)})p_1}$$

$$(3) S_{R(M2)} = \{p | \|p\|_2 \geq \tau_{(3)}, p \in \Delta_n\}$$

$$\implies \arg \min_s (p(\sigma|\varepsilon_{0:s}) \in \mathcal{R}_S) = \hat{s} > \log_\varepsilon \frac{(1 - p_1)(\tau_{(3)} + (2\tau_{(3)} - 1)^{1/2})}{(1 - \tau_{(3)})^2 p_1}$$

Proof. $p(\varepsilon_s|\sigma) \propto [\varepsilon, 1, \dots, 1] \implies p(\sigma|\varepsilon_{0:s}) \propto [p_1 \varepsilon^s, p_2, \dots, p_n]0$. WLOG assume $2 = \arg \max_{i \neq 1} p_i$;

$$\begin{aligned} (1) p(\sigma|\varepsilon_{0:s}) &\in S_{R(M1)} \\ \implies \frac{p_1 \varepsilon^s}{p_1 \varepsilon^s + p_2 + p_3 + \dots + p_n} &> \tau \\ \rightarrow \frac{p_1 \varepsilon^s}{p_1 \varepsilon^s + (1 - p_1)} &> \tau \rightarrow s > \log_\varepsilon \frac{(1 - p_1)\tau}{(1 - \tau)p_1} \\ (2) p(\sigma|\varepsilon_{0:s}) &\in S_{R(MP)} \\ \implies \frac{p_1 \varepsilon^s - p_2}{p_1 \varepsilon^s + p_2 + p_3 + \dots + p_n} &> \tau_{(2)} \\ \rightarrow \frac{p_1 \varepsilon^s - p_2}{p_1 \varepsilon^s + (1 - p_1)} &> \tau_{(2)} \rightarrow s > \log_\varepsilon \frac{(1 - p_1)\tau_{(2)} + p_2}{(1 - \tau_{(2)})p_1} \end{aligned}$$

Similar approach is applied on $\|\cdot\|_2^2$;

$$\begin{aligned} (3) p(\sigma|\varepsilon_{0:s}) &\in S_{R(M2)} \\ \implies \frac{(p_1 \varepsilon^s)^2 + p_2^2 + \dots + p_n^2}{(p_1 \varepsilon^s + (1 - p_1))^2} &\geq \tau_{(3)} \\ \rightarrow (\varepsilon^s)^2 p_1^2 (1 - \tau_{(3)}) + \varepsilon^s (-2p_1 \tau_{(3)} (1 - p_1)) &+ (p_2^2 + p_3^2 + \dots + p_n^2 - \tau_{(3)}(1 - p_1)^2) \geq 0 \end{aligned}$$

Observe that the equation above is a quadratic polynomial of ε^s and hence roots are obtained via the discriminant δ ;

$$\begin{aligned} \delta &= \left(4\tau_{(3)}^2 p_1^2 (1 - p_1)^2 - 4p_1^2 (1 - \tau_{(3)}) (p_2^2 + p_3^2 + \dots + p_n^2 - T(1 - p_1)^2) \right)^{1/2} \\ &\geq \left(4\tau_{(3)}^2 p_1^2 (1 - p_1)^2 - 4p_1^2 (1 - \tau_{(3)}) ((1 - p_1)^2 - T(1 - p_1)^2) \right)^{1/2} \\ &= 4p_1^2 (1 - p_1^2) (\tau_{(3)}^2 - (1 - \tau_{(3)})^2)^{1/2} \end{aligned}$$

$s \in \mathbb{N} \implies \delta \in \mathbb{R} \implies \tau_{(3)} > 0.5 \implies \delta \geq 2p_1^2 (1 - p_1) (2\tau - 1)^{1/2}$. From this point one can state the following;

$$\begin{aligned} \varepsilon^s &\geq \frac{2\tau_{(3)} p_1 (1 - p_1) + \delta}{2p_1^2 (1 - \tau_{(3)})^2} \\ &\geq \frac{2\tau_{(3)} p_1 (1 - p_1) + 4p_1^2 (1 - p_1^2) (\tau_{(3)}^2 - (1 - \tau_{(3)})^2)^{1/2}}{2p_1^2 (1 - \tau_{(3)})^2} \\ &= \frac{(1 - p_1)(\tau_{(3)} + (2\tau_{(3)} - 1)^{1/2})}{p_1 (1 - \tau_{(3)})^2} \\ \rightarrow s &\geq \log_\varepsilon \frac{(1 - p_1)(\tau_{(3)} + (2\tau_{(3)} - 1)^{1/2})}{p_1 (1 - \tau_{(3)})^2} \end{aligned}$$

□

Lemma 4. Following Lemma 3

$p(\sigma|\varepsilon_{0:s}) \in \Delta_n \forall s \in \{0, 1, \dots\}$ with $p(\sigma|\varepsilon_{0:s}) = p(\sigma) \oplus p(\varepsilon_0|\sigma) \oplus \dots \oplus p(\varepsilon_s|\sigma)$, and \mathcal{R}_S denotes the stopping region s.t. $(S) : p(\sigma|\varepsilon_{0:s}) \in \mathcal{R}_S$. WLOG, let 1^{th} location belong to the target class. Given $p(\varepsilon_s|\sigma) \propto [\varepsilon, 1, \dots, 1]$ where

$\varepsilon \sim \text{lognormal}(\mu, c^2)$. Let $\text{erf}(\cdot)$ denote the error function, then the following relations hold;

$$\begin{aligned}
 (1) S_{R(M1)} &= \{p | p_1 \geq \tau, p \in \Delta_n\} \\
 \implies p(p(\sigma|\varepsilon_{0:s}) \in S_{R(M1)}) &= \frac{1}{2} - \frac{1}{2} \text{erf}\left(\frac{\log(k_1) - s\mu}{\sqrt{2sc}}\right) \\
 \text{where } k_1 &= ((1 - p_1)\tau) / ((1 - \tau)p_1) \\
 (2) S_{R(MP)} &= \left\{p | p_1 - p_i \geq \tau_{(2)}, \hat{i} = \arg \max_{i \neq 1} p_i, p \in \Delta_n\right\} \\
 \implies p(p(\sigma|\varepsilon_{0:s}) \in S_{R(MP)}) &= \frac{1}{2} - \frac{1}{2} \text{erf}\left(\frac{\log(k_2) - s\mu}{\sqrt{2sc}}\right) \\
 \text{where } k_2 &= ((1 - p_1)\tau_{(2)} + p_i) / ((1 - \tau_{(2)})p_1) \\
 (3) S_{R(M2)} &= \{p | \|p\|_2 \geq \tau_{(3)}, p \in \Delta_n\} \\
 \implies p(p(\sigma|\varepsilon_{0:s}) \in S_{R(M2)}) &= \frac{1}{2} - \frac{1}{2} \text{erf}\left(\frac{\log(k_3) - s\mu}{\sqrt{2sc}}\right) \\
 \text{where } k_3 &= \frac{(1 - p_1)(\tau_{(3)} + (2\tau_{(3)} - 1)^{1/2})}{(1 - \tau_{(3)})^2 p_1}
 \end{aligned}$$

Proof. Observe the following trivial steps;

$$\begin{aligned}
 \varepsilon_i \sim \text{lognormal}(\mu, c^2) &\implies \left(\prod_{i=1}^s \varepsilon_i\right) \sim \text{lognormal}(s\mu, sc^2) \\
 p(x > y) &= 1 - p(x < y)
 \end{aligned}$$

Following the numbers obtained in Lemma3, it is trivial to calculate respective values using lognormal cdf. \square

Proof Proposition 5. Following Lemma 4

This is trivially a comparison of k_1, k_2 presented in Lemma 4. Observe the following;

$$\begin{aligned}
 &p(p(\sigma|\varepsilon_{0:s}) \in S_{R(MP)}) - p(p(\sigma|\varepsilon_{0:s}) \in S_{R(M1)}) \\
 &= \left(-\text{erf}\left(\frac{\log(k_1) - s\mu}{\sqrt{2sc}}\right)\right) - \left(-\text{erf}\left(\frac{\log(k_2) - s\mu}{\sqrt{2sc}}\right)\right)
 \end{aligned}$$

Observe that $\log(\cdot)$ and $\text{erf}(\cdot)$ are monotonically increasing. Hence $f(x) = -\text{erf}\left(\frac{\log(x) - s\mu}{\sqrt{2sc}}\right)$ is monotonically decreasing wrt. the argument x . Therefore, it is sufficient to compare $k_i \forall i$ to conclude the order between the identities. We calculate k_i wrt. τ only;

$$\begin{aligned}
 k_1 &= \frac{(1 - p_1)\tau}{(1 - \tau)p_1} \\
 k_2 &= \frac{(1 - p_1)(1 - \bar{\tau}) + p_i}{(1 - \tau_{(2)})p_1} = \frac{(1 - p_1)(2\tau - 1) + p_i}{(1 - 2\tau + 1)p_1} \\
 &= \frac{2(1 - p_1)\tau - (1 - p_1 - p_i)}{2(1 - \tau)p_1} \\
 &= \frac{(1 - p_1)\tau}{(1 - \tau)p_1} - \frac{1 - p_1 - p_i}{(1 - \tau)p_1} \rightarrow p_1 + p_i \leq 1 \implies k_2 < k_1
 \end{aligned}$$

Hence this concludes $f(k_1) < f(k_2) \implies p(p(\sigma|\varepsilon_{0:s}) \in S_{R(MP)}) > p(p(\sigma|\varepsilon_{0:s}) \in S_{R(M1)})$ implying that the probability of true selection in (MP) is higher.

Accordingly probabilities of stopping with an incorrect decision is calculated as the following; WLOG choose $i = 2$,

$$\begin{aligned}
 p(\sigma|\varepsilon_{0:s}) \in S'_{R(M1)} &\rightarrow \frac{p_2}{p_1\varepsilon + (1 - p_1)} > \tau \\
 \rightarrow \varepsilon < \frac{p_2 - (1 - p_1)\tau}{\tau p_1} &\implies p(p(\sigma|\varepsilon_{0:s}) \in S'_{R(M1)}) \\
 &= p\left(\varepsilon < \frac{p_2 - (1 - p_1)\tau}{\tau p_1}\right)
 \end{aligned}$$

False alarm probability for (MP) is calculated as the following, probability of a competitor (p_2) exceeding the probability of the target class (p_1) by the margin. We use the relation $\bar{\tau} = 2 - 2\tau$ and write the following;

$$\begin{aligned}
 p(\sigma|\varepsilon_{0:s}) \in S'_{R(MP)} &\rightarrow \frac{p_2}{p_1\varepsilon + (1 - p_1)} - \frac{p_1\varepsilon}{p_1\varepsilon + (1 - p_1)} \\
 &> (1 - \bar{\tau}) \rightarrow \frac{p_2 - (1 - p_1)(2\tau - 1)}{p_1(1 + (2\tau - 1))} > \varepsilon \\
 \rightarrow \frac{p_2 - (1 - p_1)(2\tau - 1)}{p_1(2\tau)} > \varepsilon &\implies p(p(\sigma|\varepsilon_{0:s}) \in S_{R(MP)}) \\
 &= p\left(\varepsilon < \frac{p_2 - (1 - p_1)(2\tau - 1)}{p_1(2\tau)}\right)
 \end{aligned}$$

Observe that, this happens due to p_2 being the second highest competitor in the classification task. Following previous statements, one can compare values for ε cdfs for (M1), (MP) and (MP). The probabilities are listed in the following using the definitions $\bar{\tau} = 2 - 2\tau$ and $\tilde{\tau} = \frac{(n-1)(2\tau-1)+1}{n}$;

$$\begin{aligned}
 p(p(\sigma|\varepsilon_{0:s}) \in S'_{R(M1)})(\tau) &= p\left(\varepsilon < \frac{p_2 - (1 - p_1)\tau}{\tau p_1}\right) \\
 p(p(\sigma|\varepsilon_{0:s}) \in \bar{S}_{R(MP)})(\bar{\tau}) &= p\left(\varepsilon < \frac{p_2 - (1 - p_1)(2\tau - 1)}{p_1(2\tau)}\right) \\
 &\quad p(p(\sigma|\varepsilon_{0:s}) \in S'_{R(\bar{M1})})(\tilde{\tau}) \\
 &= p\left(\varepsilon < \frac{np_2 - (1 - p_1)((n - 1)(2\tau - 1) + 1)}{((n - 1)(2\tau - 1) + 1)p_1}\right)
 \end{aligned}$$

Furthermore we define the following;

$$\begin{aligned}
 k'_1 &= \frac{p_2 - (1 - p_1)\tau}{\tau p_1} \\
 k'_2 &= \frac{p_2 - (1 - p_1)(2\tau - 1)}{p_1(2\tau)} \\
 \bar{k}'_1 &= \frac{np_2 - (1 - p_1)((n - 1)(2\tau - 1) + 1)}{((n - 1)(2\tau - 1) + 1)p_1}
 \end{aligned}$$

Observe the following relations;

$$k'_2 - k'_1 = \frac{1 - p_1 - p_2}{2\tau p_1} \geq 0 \implies k'_2 > k'_1$$

and,

$$\begin{aligned}
\frac{\delta \bar{k}'_1}{\delta n} &= \frac{2p_2(1-\tau)}{p_1(2\tau(n-1)-n+2)^2} \geq 0 \implies \frac{\bar{k}'_1}{\delta n} \Big|_{n=2} \\
\implies p_2 &= 1-p_1 \implies k'_2 = \frac{p_2 - (1-p_1)(2\tau-1)}{p_1(2\tau)} \\
&= \frac{(1-p_1)(2-2\tau)}{2p_1\tau} = \frac{(1-p_1)(1-\tau)}{\tau p_1} \\
&\& \bar{k}'_1 = \frac{2p_2 - (1-p_1)(2\tau)}{(2\tau)p_1} = \frac{(1-p_1)(1-\tau)}{\tau p_1} \\
&\rightarrow k'_2 = \bar{k}'_1 \Big|_{n=2} \implies \bar{k}'_1 > k'_2 \text{ from monotonic increasing.}
\end{aligned}$$

Therefore we conclude $\bar{k}'_1 > k'_2 > k'_1$. Similarly with the first part of the proof this implies; $p(p(\sigma|\varepsilon_{0:s}) \in S'_{R(\bar{M}_1)})(\bar{\tau}) > p(p(\sigma|\varepsilon_{0:s}) \in S_{R(MP)})(\bar{\tau}) > p(p(\sigma|\varepsilon_{0:s}) \in S'_{R(M_1)})(\tau)$ implying that the incorrect selection can be sandwiched. \square
